Performance Analysis of Power-Domain NOMA for Full-Duplex Two-Way Relaying

Volkan Ozduran, Nurul Huda Mahmood and Nikolaos Nomikos

Abstract

Non-orthogonal multiple has the potential to improve the connectivity of wireless networks by simultaneously allowing users and devices to access the wireless medium. Meanwhile, full-duplex communication can increase the spectral efficiency of the network as transmission and reception are concurrently performed. This paper investigates full-duplex two-way relay communication relying on non-orthogonal multiple access in the power-domain. More specifically, users exchange superimposed signals and perform reception by utilizing echo-cancellation and successive interference cancellation. For this setup, an extensive theoretical analysis is conducted, in terms of outage probability, error probability, ergodic rate, and throughput. Furthermore, by using the Lagrangian multiplier, optimal transmit power and power allocation coefficients are determined and the relay's position is optimized to improve network performance. Our theoretical findings are verified through Monte-Carlo simulations while significant performance gains in the optimized network case are observed.

Index Terms

Full-Duplex, Two-way Relay, PD-NOMA, Performance Analysis

I. Introduction

Non-orthogonal multiple access (NOMA) is an important technique to enhance the connectivity of fifth generation (5G) and beyond networks. Towards this end, NOMA improves spectrum utilization compared to conventional orthogonal multiple access (OMA), as multiple users are allowed to simultaneously access the wireless medium [1]. Several studies have shown the superiority of NOMA over OMA for satisfying 5G and beyond requirements in one-way relaying scenarios [2]–[5]. Moreover, the use of analog network coding enables two-way relay operation, reducing the number of time-slots required for information exchange [6]–[9]. When full-duplex (FD) relays are employed over half-duplex ones, the wireless resource efficiency is maximized, as long as loop-interference is efficiently mitigated, completing the information exchange in a single time-slot [10]–[12].

Various works have studied two-way HD NOMA relaying schemes. The works in [13], [14] focus on two user pairs exchanging information via a decode-and-forward (DF) relay and examine the impact of imperfect successive interference cancellation (SIC) on the outage performance. Performance evaluation shows that two-way NOMA relaying outperforms OMA for low signal-to-noise ratio (SNR) values while imperfect SIC results in error floors and throughput ceilings. The authors in [15] study a HD DF two-way relay network with imperfect channel state

V. Ozduran is with the Department of Electrical and Electronics Engineering, Istanbul University-Cerrahpasa, Istanbul, Turkey. N. H. Mahmood is with 6G Flagship, Centre for Wireless Communications, University of Oulu, Finland. N. Nomikos is with the IRIDA Research Center for Communication Technologies, Department of Electrical and Computer Engineering, University of Cyprus,1678 Nicosia, Cyprus. This work is partially supported by the Academy of Finland, 6G Flagship program (grant no. 346208). Corresponding e-mail: *volkan@istanbul.edu.tr*.

information (CSI), due to feedback delays, and perfect/imperfect SIC. Outage and throughput comparisons with two-way OMA reveal the gains of NOMA. The joint effect of in-phase/quadrature-phase imbalance and imperfect SIC is investigated in [16]. Performance comparisons show that NOMA exhibit reduced outages than OMA but residual interference leads to error floors and zero diversity. Then, the paper in [17] investigates two-way power line relay communication with imperfect SIC. NOMA is shown to surpass OMA's outage and ergodic rate performance, even though a rate ceiling exists due to imperfect SIC. The study in [18] considers a multi-antenna relay serving multiple user pairs under imperfect CSI. Both delay-constrained and delay-tolerant scenarios are investigated, showing that NOMA better exploits rate differences and serves more users than OMA. The impact of imperfect SIC when a user acts as a two-way relay for a cell-edge user is studied in [19]. Outage, ergodic sum rate and energy efficiency analysis is conducted and an efficient power allocation scheme is presented, based on segment and particle swarm optimization. In [20], the optimal information exchanging user set for ergodic sum capacity is examined, under perfect and imperfect SIC, revealing large capacity gains in the two-way NOMA relay case over OMA. The joint power and time optimization in a three-phase two-way NOMA relay scheme for two users is presented in [21]. Comparisons with other power and time allocation schemes and conventional one-way NOMA highlight outage and ergodic rate gains for the proposed scheme. The work in [22] considers a two-user NOMA relay network where users transmit in the first two phases while in the third phase, the relay applies superposition coding and transmits a network-coded symbol to the users. Analytical and simulation results show that the proposed scheme outperforms two-phase and four-phase alternatives in terms of average achievable rate. In cases where multiple user pairs exist, a relay equipped with a massive number of antennas, the authors in [23] show that it can support end-to-end communication for all the pairs, over two-time slots. The gains of NOMA in two-way vehicular networks are demonstrated in [24] where the sum outage probability performance is shown to outperform two-way OMA. The secrecy performance of NOMA in a two-way relay network with an eavesdropper is investigated in [25], concluding that NOMA is superior to OMA, in terms of secrecy, as the eavesdropper must decode the combined signal which is broadcasted from the relay.

Other works study the performance of two-way NOMA when a FD relay is available. In [26], the system outage performance is investigated Nakagami-m fading, highlighting the efficiency of FD NOMA when low transmit power is used HD NOMA and FD OMA. The outage performance in scenarios where co-channel interference affects the reception of users and the relay is investigated in [27]. Performance analysis highlights throughput gains for FD relaying over HD relaying under perfect and imperfect SIC. The impact of imperfect SIC is also examined in [28] for underwater acoustic sensor networks. Analytical and simulation results reveal that in such networks, two-way FD NOMA relaying can improve both communication reliability and energy efficiency. In settings where a user acts a FD two-way relay for a cell-edge user, the paper in [29] presents on/off FD and HD relaying schemes. The activation of cooperative relaying, complementing direct communication is decided through an on/off mechanism. Outage and throughput results suggest that the FD relaying outperforms HD relaying in the low SNR regime. When a wireless power FD relay exists, the work in [30] studies two-way user cooperation and proposes a time-switching protocol for energy and information transmission. Results show that a higher time-split factor improves the outage performance of the cell-edge user at low SNR, while at the high SNR a lower time-split factor is needed to reduce

the impact of LI at the relay and maintain low outages. Another study in [31] focuses on wireless power relaying and proposes a power splitting protocol to improve the energy harvesting efficiency and the overall performance of two-way FD NOMA.

In other cases, multiple relays might be available to provide additional diversity when performing two-way NOMA communication. In a network with two and two users communicating with a base station, the authors in [32] studied the sum-rate performance of HD two-way NOMA relaying, revealing improved performance over OMA. Another work proposing two-way NOMA with two relays is [33]. Here, users are to different relays, due to the blockage and the sum-rate performance of the proposed two time-slot protocol is analyzed, suggesting gains over OMA and NOMA alternatives. The works in [34], [35] present multiple access broadcast NOMA and time division broadcast NOMA and perform joint antenna and relay selection, increasing the diversity of the multi-relay NOMA network. Other works presenting opportunistic relay selection in two-way NOMA networks and enabling the relay to perform digital network coding are [36], [37]. In the considered topologies, the outage performance was improved by activating the relay according to max-min SINR criteria. A variation of the opportunistic relay selection problem was presented in [38] taking into consideration the hardware impairments at the relay. More specifically, the selecting criterion is based on choosing the relay the highest signal-to-interference-plus-noise-and-distortion ratio. The practical issues of imperfect CSI and SIC when selecting the best relay are considered in [39], selecting a relay according to the maximum estimated channel gains. Finally, in an FD multi-relay network, the study in [40] employs rate splitting and successive group decoding, leveraging the interference signals from neighboring users. Performance results, in terms of ergodic rate and outrage probability highlight the improvements of the proposed NOMA scheme over OMA.

Motivated from the increased potential of combining NOMA and FD two-way relaying, this paper studies a cooperative network where an FD amplify-and-forward (AF) relay establishes the connectivity among two users through the NOMA paradigm. Such a setup can correspond to a wireless sensor network, in the context of the Internet-of-Things (IoT). An illustrative example involves two IoT sensors exchanging their measurements, such as moisture and potassium soil levels through a more advanced relay terminal determining the power allocation for NOMA. Contrary to other relevant studies, we consider at the same time, the detrimental effect of LI at the users and the relay and the use of SIC and echo cancellation to retrieve the information signals. Also, this paper tackles a more complex problem, i.e. two-way communication, compared to our previous work in [5], studying one-way FD NOMA relaying. In greater detail, this paper provides the following contributions:

- As FD user and relay terminals are assumed, users employ echo cancellation to retrieve their desired information signals from the combined signal that is broadcasted by the relay. Meanwhile, the relay adopts SIC to correctly separate the information signals of the users.
- A thorough theoretical analysis is conducted, in terms of outage probability (OP), error probability (EP), ergodic rate (ER), and throughput, deriving analytical and asymptotic expressions.
- Aiming to further enhance the performance of FD two-way NOMA relay networks, we optimize the transmit power and power allocation coefficients under fixed relay position. Moreover, when fixed resource allocation is assumed, we optimize the relay location

- Our analytical findings are verified through Monte-Carlo simulations and the performance gains from the proposed optimization process are clearly depicted over the non-optimized case.

The structure of this work is as follows. Section 2 provides details on the system model and channel statistics. Then, Section 3 presents the theoretical performance analysis of the two-way relay network while the optimization procedure is given in Section 4. Our theoretical results are verified through Monte-Carlo simulations in Section 5 and finally, conclusions and future directions are given in Section 6.

Table I includes a list of acronyms used in this paper.

TABLE I: List of acronyms

5G	Fifth generation
AF	Amplify-and-forward
AWGN	Additive white Gaussian noise
BPSK	Binary phase-shift keying
CDF	Cumulative density function
CSI	Channel state information
DF	Decode-and-forward
EP	Error probability
ER	Ergodic rate
FD	Full-duplex
HD	Half-duplex
IoT	Internet-of-Things
LI	Loop-interference
NOMA	Non-orthogonal multiple access
OMA	Orthogonal multiple access
OP	Outage probability
PDF	Probability density function
QPSK	Quadrature phase-shift keying
SIC	Successive interference cancellation
SINR	Signal-to-interference-plus-noise ratio
SNR	Signal-to-noise ratio

Notations: The terms $f_h(.)$ and $F_h(.)$ represent the probability density function (PDF) and cumulative distribution function (CDF) of a random variable (RV) h, respectively. The operators $\mathbb{E}[.]$ and $\Pr(.)$ represent the expectation and probability, respectively. $G_{p,q}^{m,n}[.]$ is the Meijer's G-function [41, Eq. (21)] and $G_{p,q:p_1,q_1:p_2,q_2}^{m,n:m_1,n_1:m_2,n_2}[.]$ is the extended generalized bi-variate Meijer's G-function [42, Eq. (13)]. All log are base 2 unless stated otherwise and $\Gamma(.)$ is the complete Gamma function [43, Eq. (8.310.1)].

II. System Model and Channel Statistics

Figure 1 presents a two-hop NOMA-based FD two-way relaying network. S_1 and S_2 conduct information exchange with the help of a single FD relay terminal. S_1 and S_2 do not have a direct-link due to excessive fading and shadowing conditions. Since the relay and the user terminals operate in FD mode, the information exchange process requires a single time-slot. The channel impulse responses between $S_1 \longrightarrow$ relay and $S_2 \longrightarrow$ relay are denoted as h and g, respectively. The h and g are complex Gaussian RVs with zero mean and variances σ_h^2 and σ_g^2, respectively, i.e. $h \sim \mathcal{CN}\left(0, \sigma_h^2\right)$ and $g \sim \mathcal{CN}\left(0, \sigma_g^2\right)$. Also, a, $a \sim \mathcal{CN}\left(0, \sigma_a^2\right)$, b, $b \sim \mathcal{CN}\left(0, \sigma_b^2\right)$ and c, $c \sim \mathcal{CN}\left(0, \sigma_c^2\right)$ are LI at

S_1, relay and S_2, respectively. Finally, Rayleigh block fading is considered with channels remaining static during the duration of a time-slot.

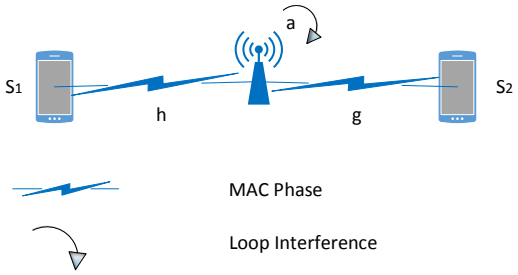

Fig. 1: A two-hop NOMA-based FD two-way wireless relaying network.

S_1 and S_2 simultaneously transmit their information signals via non-orthogonal channels and the received signal at the relay can be written as:

$$Z_r = h\left(\sqrt{\alpha_1 \mathrm{P}_{s1}}x_1 + \sqrt{\alpha_2 \mathrm{P}_{s1}}x_2\right) + g\left(\sqrt{\beta_1 \mathrm{P}_{s2}}y_1 + \sqrt{\beta_2 \mathrm{P}_{s2}}y_2\right) + \sqrt{\mathrm{P}_r}b + n_r \tag{1}$$

where P_{s1}, P_{s2}, and P_r are the corresponding transmit powers of S_1, S_2, and relay terminal, respectively. n_r is the additive white Gaussian noise (AWGN) at relay. α_i and β_i, $\forall_i = 1, 2$ are the power allocation coefficients, where $\alpha_1 + \alpha_2 = 1$, $\alpha_1 > \alpha_2$ and $\beta_1 + \beta_2 = 1$, $\beta_1 > \beta_2$. The order of power allocation coefficients is formulated as: $\alpha_2 \leq \beta_2 < \alpha_1 \leq \beta_1$. Since the relay terminal operates in AF mode, the variable gain based G amplification factor can be obtained as

$$G = \sqrt{\frac{\mathrm{P}_r}{\mathrm{P}_{s1}|h|^2\left(\alpha_1 + \alpha_2\right) + \mathrm{P}_{s2}|g|^2\left(\beta_1 + \beta_2\right) + \mathrm{P}_r|b|^2 + \sigma^2}}. \tag{2}$$

The received amplified signals at S_1 and S_2 can be written as in (3) and (4), respectively.

$$y_{S_1} = G\left(h\left(\sqrt{\alpha_1 \mathrm{P}_{s1}}x_1 + \sqrt{\alpha_2 \mathrm{P}_{s1}}x_2\right) + g\left(\sqrt{\beta_1 \mathrm{P}_{s2}}y_1 + \sqrt{\beta_2 \mathrm{P}_{s2}}y_2\right) + \sqrt{\mathrm{P}_r}b + n_r\right)h + \sqrt{\mathrm{P}_{s1}}a + n_{s_1}, \tag{3}$$

$$y_{S_2} = G\left(h\left(\sqrt{\alpha_1 \mathrm{P}_{s1}}x_1 + \sqrt{\alpha_2 \mathrm{P}_{s1}}x_2\right) + g\left(\sqrt{\beta_1 \mathrm{P}_{s2}}y_1 + \sqrt{\beta_2 \mathrm{P}_{s2}}y_2\right) + \sqrt{\mathrm{P}_r}b + n_r\right)g + \sqrt{\mathrm{P}_{s2}}c + n_{s_2}. \tag{4}$$

where n_{s_1} and n_{s_2} are the AWGN at S_1 and S_2, respectively. By using successive interference and echo cancellations, the achievable rates, R_{y_1} and R_{y_2}, at S_1 can be calculated as

$$R_{y_1}^{S_1} = \log\left(1 + \frac{G^2|h|^2|g|^2\beta_1 \mathrm{P}_{s2}}{G^2|h|^2|g|^2\beta_2 \mathrm{P}_{s2} + G^2|h|^2\mathrm{P}_r|b|^2 + G^2|h|^2\sigma^2 + \mathrm{P}_{s1}|a|^2 + \sigma^2}\right) \tag{5}$$

$$R_{y_2}^{S_1} = \log\left(1 + \frac{G^2|h|^2|g|^2\beta_2 \mathrm{P}_{s2}}{G^2|h|^2\mathrm{P}_r|b|^2 + G^2|h|^2\sigma^2 + \mathrm{P}_{s1}|a|^2 + \sigma^2}\right) \tag{6}$$

Substituting the G amplification factor, (2), into (5) and (6) and performing some mathematical processes, (5) and

(6) can be re-written as:

$$R_{y_1}^{S_1} = \log\left(1 + \frac{\frac{\varphi\gamma_x\gamma_y\beta_1}{[\gamma_a+1][\gamma_b+1]}}{\frac{\varphi\gamma_x}{[\gamma_a+1]} + \frac{\gamma_x(\alpha_1+\alpha_2)+\gamma_y(\beta_1+\beta_2)}{[\gamma_b+1]} + \frac{\varphi\gamma_x+\varphi\gamma_x\gamma_y\beta_2+\gamma_x(\alpha_1+\alpha_2)+\gamma_y(\beta_1+\beta_2)}{[\gamma_a+1][\gamma_b+1]} + 1}\right), \tag{7}$$

$$R_{y_2}^{S_1} = \log\left(1 + \frac{\frac{\varphi\gamma_x\gamma_y\beta_2}{[\gamma_a+1][\gamma_b+1]}}{\frac{\varphi\gamma_x}{[\gamma_a+1]} + \frac{\gamma_x(\alpha_1+\alpha_2)+\gamma_y(\beta_1+\beta_2)}{[\gamma_b+1]} + \frac{\varphi\gamma_x+\gamma_x(\alpha_1+\alpha_2)+\gamma_y(\beta_1+\beta_2)}{[\gamma_a+1][\gamma_b+1]} + 1}\right), \tag{8}$$

where $\gamma_x = \frac{\mathrm{P}_{s1}|h|^2}{\sigma^2}$, $\gamma_y = \frac{\mathrm{P}_{s2}|g|^2}{\sigma^2}$, $\gamma_a = \frac{\mathrm{P}_{s1}|a|^2}{\sigma^2}$, $\gamma_b = \frac{\mathrm{P}_r|b|^2}{\sigma^2}$, and $\varphi = \frac{\mathrm{P}_r}{\mathrm{P}_{s1}=\mathrm{P}_{s2}}$ [44]. Following the same procedures, the achievable rate expressions at S_2, which are $R_{x_1}^{S_2}$ and $R_{x_2}^{S_2}$, can be calculated as

$$R_{x_1}^{S_2} = \log\left(1 + \frac{\frac{\varphi\gamma_x\gamma_y\alpha_1}{[\gamma_b+1][\gamma_c+1]}}{\frac{\varphi\gamma_y}{[\gamma_c+1]} + \frac{\gamma_x(\alpha_1+\alpha_2)+\gamma_y(\beta_1+\beta_2)}{[\gamma_b+1]} + \frac{\varphi\gamma_x\gamma_y\alpha_2+\varphi\gamma_y+\gamma_x(\alpha_1+\alpha_2)+\gamma_y(\beta_1+\beta_2)}{[\gamma_b+1][\gamma_c+1]} + 1}\right), \tag{9}$$

$$R_{x_2}^{S_2} = \log\left(1 + \frac{\frac{\varphi\gamma_x\gamma_y\alpha_2}{[\gamma_b+1][\gamma_c+1]}}{\frac{\varphi\gamma_y}{[\gamma_c+1]} + \frac{\gamma_x(\alpha_1+\alpha_2)+\gamma_y(\beta_1+\beta_2)}{[\gamma_b+1]} + \frac{\varphi\gamma_y+\gamma_x(\alpha_1+\alpha_2)+\gamma_y(\beta_1+\beta_2)}{[\gamma_b+1][\gamma_c+1]} + 1}\right), \tag{10}$$

where $\gamma_c = \frac{\mathrm{P}_{s2}|c|^2}{\sigma^2}$.

III. Performance Analysis

OP, EP, ER and throughput analytical and asymptotic derivations are presented in this section.

A. Outage Probability

The OP is the probability that the achievable rate falls below the pre-defined target rate, R, expressed in bps/Hz. By using the logarithm properties, the OP is the CDF of received Signal-to-noise ratio (SNR)/Signal-to-interference-plus-noise ratio (SINR) evaluated at the target threshold rate, γ_{th} [45]. Since the forms of (7), (8), (9), and (10) are

intractable, this paper upper-bounds of these expressions are given with the help of $\frac{\mathrm{AB}}{\mathrm{A+B}} \leq \min(\mathrm{A},\mathrm{B})$ structure as

$$\begin{aligned}
\gamma_{y_1}^{S_1} &= \frac{\varphi\gamma_x\gamma_y\beta_1}{\gamma_x\left(\varphi\gamma_y\beta_2+\varphi\gamma_B+\gamma_A(\alpha_1+\alpha_2)+\varphi+(\alpha_1+\alpha_2)\right)+\gamma_y(\gamma_A(\beta_1+\beta_2)+(\beta_1+\beta_2))} \\
&= \frac{\frac{\varphi\gamma_x\gamma_y\beta_1}{(\gamma_A(\beta_1+\beta_2)+(\beta_1+\beta_2))\left(\varphi\gamma_y\beta_2+\varphi\gamma_B+\gamma_A(\alpha_1+\alpha_2)+\varphi+(\alpha_1+\alpha_2)\right)}}{\frac{\gamma_x}{(\gamma_A(\beta_1+\beta_2)+(\beta_1+\beta_2))}+\frac{\gamma_y}{\left(\varphi\gamma_y\beta_2+\varphi\gamma_B+\gamma_A(\alpha_1+\alpha_2)+\varphi+(\alpha_1+\alpha_2)\right)}} \\
&= \varphi\beta_1\frac{AB}{A+B} \leq \gamma_{y_1}^{S_1\mathrm{up}} = \varphi\beta_1\min(\mathrm{A},\mathrm{B}), \qquad (11)
\end{aligned}$$

$$\begin{aligned}
\gamma_{y_2}^{S_1} &= \frac{\varphi\gamma_x\gamma_y\beta_2}{\gamma_x(\varphi\gamma_B+\gamma_A(\alpha_1+\alpha_2)+\varphi+(\alpha_1+\alpha_2))+\gamma_y(\gamma_A(\beta_1+\beta_2)+(\beta_1+\beta_2))} \\
&= \frac{\frac{\varphi\gamma_x\gamma_y\beta_2}{(\gamma_A(\beta_1+\beta_2)+(\beta_1+\beta_2))(\varphi\gamma_B+\gamma_A(\alpha_1+\alpha_2)+\varphi+(\alpha_1+\alpha_2))}}{\frac{\gamma_x}{(\gamma_A(\beta_1+\beta_2)+(\beta_1+\beta_2))}+\frac{\gamma_y}{(\varphi\gamma_B+\gamma_A(\alpha_1+\alpha_2)+\varphi+(\alpha_1+\alpha_2))}} \\
&= \varphi\beta_2\frac{AC}{A+C} \leq \gamma_{y_2}^{S_1\mathrm{up}} = \varphi\beta_2\min(\mathrm{A},\mathrm{C}), \qquad (12)
\end{aligned}$$

$$\begin{aligned}
\gamma_{x_1}^{S_2} &= \frac{\varphi\gamma_x\gamma_y\alpha_1}{\gamma_x(\gamma_C(\alpha_1+\alpha_2)+(\alpha_1+\alpha_2))+\gamma_y(\varphi\gamma_x\alpha_2+\varphi\gamma_B+\gamma_C(\beta_1+\beta_2)+\varphi+(\beta_1+\beta_2))} \\
&= \frac{\frac{\varphi\gamma_x\gamma_y\alpha_1}{(\varphi\gamma_x\alpha_2+\varphi\gamma_B+\gamma_C(\beta_1+\beta_2)+\varphi+(\beta_1+\beta_2))(\gamma_C(\alpha_1+\alpha_2)+(\alpha_1+\alpha_2))}}{\frac{\gamma_x}{(\varphi\gamma_x\alpha_2+\varphi\gamma_B+\gamma_C(\beta_1+\beta_2)+\varphi+(\beta_1+\beta_2))}+\frac{\gamma_y}{(\gamma_C(\alpha_1+\alpha_2)+(\alpha_1+\alpha_2))}} \\
&= \varphi\alpha_1\frac{WZ}{W+Z} \leq \gamma_{x_1}^{S_2\mathrm{up}} = \varphi\alpha_1\min(\mathrm{W},\mathrm{Z}), \qquad (13)
\end{aligned}$$

$$\begin{aligned}
\gamma_{x_2}^{S_2} &= \frac{\varphi\gamma_x\gamma_y\alpha_2}{\gamma_x(\gamma_C(\alpha_1+\alpha_2)+(\alpha_1+\alpha_2))+\gamma_y(\varphi\gamma_B+\gamma_C(\beta_1+\beta_2)+\varphi+(\beta_1+\beta_2))} \\
&= \frac{\frac{\varphi\gamma_x\gamma_y\alpha_2}{(\varphi\gamma_B+\gamma_C(\beta_1+\beta_2)+\varphi+(\beta_1+\beta_2))(\gamma_C(\alpha_1+\alpha_2)+(\alpha_1+\alpha_2))}}{\frac{\gamma_x}{(\varphi\gamma_B+\gamma_C(\beta_1+\beta_2)+\varphi+(\beta_1+\beta_2))}+\frac{\gamma_y}{(\gamma_C(\alpha_1+\alpha_2)+(\alpha_1+\alpha_2))}} \\
&= \varphi\alpha_2\frac{QZ}{Q+Z} \leq \gamma_{x_2}^{S_2\mathrm{up}} = \varphi\alpha_2\min(\mathrm{Q},\mathrm{Z}), \qquad (14)
\end{aligned}$$

where $A = \frac{\gamma_x}{(\gamma_A(\beta_1+\beta_2)+(\beta_1+\beta_2))}$, $B = \frac{\gamma_y}{\left(\varphi\gamma_y\beta_2+\varphi\gamma_B+\gamma_A(\alpha_1+\alpha_2)+\varphi+(\alpha_1+\alpha_2)\right)}$, $C = \frac{\gamma_y}{(\varphi\gamma_B+\gamma_A(\alpha_1+\alpha_2)+\varphi+(\alpha_1+\alpha_2))}$,
$W = \frac{\gamma_x}{(\varphi\gamma_x\alpha_2+\varphi\gamma_B+\gamma_C(\beta_1+\beta_2)+\varphi+(\beta_1+\beta_2))}$, $Z = \frac{\gamma_y}{(\gamma_C(\alpha_1+\alpha_2)+(\alpha_1+\alpha_2))}$, $Q = \frac{\gamma_x}{(\varphi\gamma_B+\gamma_C(\beta_1+\beta_2)+\varphi+(\beta_1+\beta_2))}$,
$\gamma_A = \gamma_a + 1$, $\gamma_B = \gamma_b + 1$, and $\gamma_C = \gamma_c + 1$.

Proposition 1. *$F_{\gamma_{y_1}}^{S_1up}$, $F_{\gamma_{y_2}}^{S_1up}$, $F_{\gamma_{x_1}}^{S_2up}$, and $F_{\gamma_{x_2}}^{S_2up}$ can be calculated as*

$$F_{\gamma_{y_1}}^{\mathrm{S_1up}}(\gamma_{\mathrm{th}}) = 1 - e^{-\gamma_{\mathrm{th}}\left(\frac{2(\beta_1+\beta_2)}{\varphi\beta_1 P_{s1}\Omega_h}+\frac{2\varphi+2(\alpha_1+\alpha_2)}{\varphi(\beta_1-\gamma_{th}\beta_2)P_{s2}\Omega_g}\right)}\frac{1}{P_{s1}\Omega_a}\left(\frac{(\beta_1+\beta_2)\gamma_{\mathrm{th}}}{\varphi\beta_1 P_{s1}\Omega_h}+\frac{(\alpha_1+\alpha_2)\gamma_{\mathrm{th}}}{\varphi\left(\beta_1-\gamma_{th}\beta_2\right)P_{s2}\Omega_g}+\frac{1}{P_{s1}\Omega_a}\right)^{-1}$$
$$\times\frac{1}{P_r\Omega_b}\left(\frac{\varphi\gamma_{\mathrm{th}}}{\varphi\left(\beta_1-\gamma_{th}\beta_2\right)P_{s2}\Omega_g}+\frac{1}{P_r\Omega_b}\right)^{-1}, \tag{15}$$

$$F_{\gamma_{y_2}}^{\mathrm{S_1up}}(\gamma_{\mathrm{th}}) = 1 - e^{-\gamma_{\mathrm{th}}\left(\frac{2(\beta_1+\beta_2)}{\varphi\beta_2 P_{s1}\Omega_h}+\frac{2\varphi+2(\alpha_1+\alpha_2)}{\varphi\beta_2 P_{s2}\Omega_g}\right)}\frac{1}{P_{s1}\Omega_a}\left(\frac{(\beta_1+\beta_2)\gamma_{\mathrm{th}}}{\varphi\beta_2 P_{s1}\Omega_h}+\frac{(\alpha_1+\alpha_2)\gamma_{\mathrm{th}}}{\varphi\beta_2 P_{s2}\Omega_g}+\frac{1}{P_{s1}\Omega_a}\right)^{-1}$$
$$\times\frac{1}{P_r\Omega_b}\left(\frac{\gamma_{\mathrm{th}}}{\beta_2 P_{s2}\Omega_g}+\frac{1}{P_r\Omega_b}\right)^{-1}, \tag{16}$$

$$F_{\gamma_{x_1}}^{\mathrm{S_2up}}(\gamma_{\mathrm{th}}) = 1 - e^{-\gamma_{\mathrm{th}}\left(\frac{2\varphi+2(\beta_1+\beta_2)}{\varphi(\alpha_1-\gamma_{th}\alpha_2)P_{s1}\Omega_h}+\frac{2(\alpha_1+\alpha_2)}{\varphi\alpha_1 P_{s2}\Omega_g}\right)}\frac{1}{P_{s2}\Omega_c}\left(\frac{\gamma_{\mathrm{th}}(\beta_1+\beta_2)}{\varphi\left(\alpha_1-\gamma_{th}\alpha_2\right)P_{s1}\Omega_h}+\frac{(\alpha_1+\alpha_2)\gamma_{\mathrm{th}}}{\varphi\alpha_1 P_{s2}\Omega_g}+\frac{1}{P_{s2}\Omega_c}\right)^{-1}$$
$$\times\frac{1}{P_r\Omega_b}\left(\frac{\varphi\gamma_{\mathrm{th}}}{\varphi\left(\alpha_1-\gamma_{th}\alpha_2\right)P_{s1}\Omega_h}+\frac{1}{P_r\Omega_b}\right)^{-1}, \tag{17}$$

$$F_{\gamma_{x_2}}^{\mathrm{S_2up}}(\gamma_{\mathrm{th}}) = 1 - e^{-\gamma_{\mathrm{th}}\left(\frac{2\varphi+2(\beta_1+\beta_2)}{\varphi\alpha_2 P_{s1}\Omega_h}+\frac{2(\alpha_1+\alpha_2)}{\varphi\alpha_2 P_{s2}\Omega_g}\right)}\frac{1}{P_{s2}\Omega_c}\left(\frac{(\beta_1+\beta_2)\gamma_{\mathrm{th}}}{\varphi\alpha_2 P_{s1}\Omega_h}+\frac{(\alpha_1+\alpha_2)\gamma_{\mathrm{th}}}{\varphi\alpha_2 P_{s2}\Omega_g}+\frac{1}{P_{s2}\Omega_c}\right)^{-1}$$
$$\times\frac{1}{P_r\Omega_b}\left(\frac{\gamma_{\mathrm{th}}}{\alpha_2 P_{s1}\Omega_h}+\frac{1}{P_r\Omega_b}\right)^{-1}, \tag{18}$$

where Ω_h, Ω_g, Ω_a, Ω_b, and Ω_c are the means of $|h|^2$, $|g|^2$, $|a|^2$, $|b|^2$, and $|c|^2$, respectively.

Proof. See Appendix A. □

B. Error Probability

The EP performance analysis is presented in this subsection. In this regard, the CDF-based EP formula [44, Eq. (25)] is considered for the analytical derivations.

$$\bar{P_e} = \frac{a_1}{2}\sqrt{\frac{b_1}{\pi}}\int_0^\infty \frac{\exp\left(-\mathrm{b_1 x}\right)}{\sqrt{x}}F(x)dx, \tag{19}$$

where $a_1 = b_1 = 1$ represents the Binary phase-shift keying (BPSK) and $a_1 = b_1 = 2$ represents the Quadrature phase-shift keying (QPSK) modulations. BPSK modulation is considered for the performance analysis. $\bar{P}_{e\,\gamma_{y_2}}^{\mathrm{S_1up}}$ and $\bar{P}_{e\,\gamma_{x_2}}^{\mathrm{S_2up}}$ are given in Proposition 2 below.

Proposition 2. *$\bar{P}_{e_{\gamma_{y_2}}}^{\mathrm{S_1up}}$ and $\bar{P}_{e_{\gamma_{x_2}}}^{\mathrm{S_2up}}$ can be calculated as*

$$\bar{P}_{e_{\gamma_{y_2}}}^{\mathrm{S_1up}} = \frac{1}{2\sqrt{\pi}}\Bigg[\sqrt{\pi} - \left(1 + \frac{2\left(\beta_1+\beta_2\right)}{\varphi\beta_2 P_{s1}\Omega_h} + \frac{2\varphi + 2\left(\alpha_1+\alpha_2\right)}{\varphi\beta_2 P_{s2}\Omega_g}\right)^{-\frac{1}{2}} \times G_{1,0:1,1:1,1}^{1,0:1,1:1,1}\left(\frac{\frac{1}{2}}{-} \,\middle|\, \begin{matrix}0\\0\end{matrix} \,\middle|\, \begin{matrix}0\\0\end{matrix} \,\middle|\, \frac{\left(\frac{\left((\beta_1+\beta_2)\varphi\beta_2 P_{s2}\Omega_g + (\alpha_1+\alpha_2)\varphi\beta_2 P_{s1}\Omega_h\right)P_{s1}\Omega_a}{\varphi^2\beta_2^2 P_{s2}\Omega_g P_{s1}\Omega_h}\right)}{\left(1 + \frac{2(\beta_1+\beta_2)}{\varphi\beta_2 P_{s1}\Omega_h} + \frac{2\varphi+2(\alpha_1+\alpha_2)}{\varphi\beta_2 P_{s2}\Omega_g}\right)}, \frac{\left(\frac{P_r\Omega_b}{\beta_2 P_{s2}\Omega_g}\right)}{\left(1 + \frac{2(\beta_1+\beta_2)}{\varphi\beta_2 P_{s1}\Omega_h} + \frac{2\varphi+2(\alpha_1+\alpha_2)}{\varphi\beta_2 P_{s2}\Omega_g}\right)}\right)\Bigg] \tag{20}$$

$$\bar{P}_{e_{\gamma_{x_2}}}^{\mathrm{S_2up}} = \frac{1}{2\sqrt{\pi}}\Bigg[\sqrt{\pi} - \left(1 + \frac{2\varphi + 2\left(\beta_1+\beta_2\right)}{\varphi\alpha_2 P_{s1}\Omega_h} + \frac{2\left(\alpha_1+\alpha_2\right)}{\varphi\alpha_2 P_{s2}\Omega_g}\right)^{-\frac{1}{2}} \times G_{1,0:1,1:1,1}^{1,0:1,1:1,1}\left(\frac{\frac{1}{2}}{-} \,\middle|\, \begin{matrix}0\\0\end{matrix} \,\middle|\, \begin{matrix}0\\0\end{matrix} \,\middle|\, \frac{\left(\frac{\left((\beta_1+\beta_2)\varphi\alpha_2 P_{s2}\Omega_g + (\alpha_1+\alpha_2)\varphi\alpha_2 P_{s1}\Omega_h\right)P_{s2}\Omega_c}{\varphi^2\alpha_2^2 P_{s2}\Omega_g P_{s1}\Omega_h}\right)}{\left(1 + \frac{2\varphi+2(\beta_1+\beta_2)}{\varphi\alpha_2 P_{s1}\Omega_h} + \frac{2(\alpha_1+\alpha_2)}{\varphi\alpha_2 P_{s2}\Omega_g}\right)}, \frac{\left(\frac{P_r\Omega_b}{\alpha_2 P_{s1}\Omega_h}\right)}{\left(1 + \frac{2\varphi+2(\beta_1+\beta_2)}{\varphi\alpha_2 P_{s1}\Omega_h} + \frac{2(\alpha_1+\alpha_2)}{\varphi\alpha_2 P_{s2}\Omega_g}\right)}\right)\Bigg] \tag{21}$$

Proof. See Appendix B. □

C. Ergodic Rate

This subsection presents the ER performance analysis. Considering [46, Eq. (32)] and adjusting it to the FD mode, the achievable rate expression can be obtained as

$$\mathrm{ER} = \frac{1}{\ln 2}\int_0^\infty \frac{1 - \mathrm{F}\left(\gamma_{\mathrm{th}}\right)}{1+\gamma_{\mathrm{th}}}\mathrm{d}\gamma_{\mathrm{th}}, \tag{22}$$

where $R_{X_1}^{\mathrm{up}} = \frac{1}{\ln 2}\int_0^\infty \frac{1-\mathrm{F}_{\gamma_{X_1}}^{\mathrm{up}}(\gamma_{\mathrm{th}})}{1+\gamma_{\mathrm{th}}}\mathrm{d}\gamma_{\mathrm{th}}$ and $R_{X_2}^{\mathrm{up}} = \frac{1}{\ln 2}\int_0^\infty \frac{1-\mathrm{F}_{\gamma_{X_2}}^{\mathrm{up}}(\gamma_{\mathrm{th}})}{1+\gamma_{\mathrm{th}}}\mathrm{d}\gamma_{\mathrm{th}}$ [46, Eq. (38)]. By plugging the related CDF expressions into the ER formula, $ER_{\gamma_{y_2}}^{\mathrm{S_1up}}$ and $ER_{\gamma_{x_2}}^{\mathrm{S_2up}}$ can be calculated as in the Proposition 3 below.

Proposition 3. *$ER_{\gamma_{y_2}}^{\mathrm{S_1up}}$ and $ER_{\gamma_{x_2}}^{\mathrm{S_2up}}$ can be calculated as*

$$\begin{aligned} ER_{\gamma_{y_2}}^{\mathrm{S_1up}} = \frac{1}{\ln 2}\Bigg[& \mathrm{B}_1\left(\frac{2\left(\beta_1+\beta_2\right)}{\varphi\beta_2\mathrm{P_{s1}}\Omega_{\mathrm{h}}} + \frac{2\varphi+2\left(\alpha_1+\alpha_2\right)}{\varphi\beta_2\mathrm{P_{s2}}\Omega_{\mathrm{g}}}\right)^{-1} \mathrm{G}_{2,1}^{1,2}\left(\frac{\frac{\left((\beta_1+\beta_2)\varphi\beta_2\mathrm{P_{s2}}\Omega_{\mathrm{g}} + (\alpha_1+\alpha_2)\varphi\beta_2\mathrm{P_{s1}}\Omega_{\mathrm{h}}\right)\mathrm{P_{s1}}\Omega_{\mathrm{a}}}{\varphi^2\beta_2^2\mathrm{P_{s1}}\Omega_{\mathrm{h}}\mathrm{P_{s2}}\Omega_{\mathrm{g}}}}{\left(\frac{2(\beta_1+\beta_2)}{\varphi\beta_2\mathrm{P_{s1}}\Omega_{\mathrm{h}}} + \frac{2\varphi+2(\alpha_1+\alpha_2)}{\varphi\beta_2\mathrm{P_{s2}}\Omega_{\mathrm{g}}}\right)}\middle|\begin{matrix}0,0\\0,-\end{matrix}\right) \\ & + B_2\left(\frac{2\left(\beta_1+\beta_2\right)}{\varphi\beta_2 P_{s1}\Omega_h} + \frac{2\varphi+2\left(\alpha_1+\alpha_2\right)}{\varphi\beta_2 P_{s2}\Omega_g}\right)^{-1} G_{2,1}^{1,2}\left(\frac{\frac{P_r\Omega_b}{\beta_2 P_{s2}\Omega_g}}{\left(\frac{2(\beta_1+\beta_2)}{\varphi\beta_2 P_{s1}\Omega_h} + \frac{2\varphi+2(\alpha_1+\alpha_2)}{\varphi\beta_2 P_{s2}\Omega_g}\right)}\middle|\begin{matrix}0,0\\0,-\end{matrix}\right) \\ & + B_3\left(\frac{2\left(\beta_1+\beta_2\right)}{\varphi\beta_2 P_{s1}\Omega_h} + \frac{2\varphi+2\left(\alpha_1+\alpha_2\right)}{\varphi\beta_2 P_{s2}\Omega_g}\right)^{-1} G_{2,1}^{1,2}\left(\frac{1}{\left(\frac{2(\beta_1+\beta_2)}{\varphi\beta_2 P_{s1}\Omega_h} + \frac{2\varphi+2(\alpha_1+\alpha_2)}{\varphi\beta_2 P_{s2}\Omega_g}\right)}\middle|\begin{matrix}0,0\\0,-\end{matrix}\right), \end{aligned} \tag{23}$$

$$ER_{\gamma_{x_2}}^{\mathrm{S_2up}} = \frac{1}{\ln 2}\Bigg[\mathrm{B}_4\left(\frac{2\varphi+2\left(\beta_1+\beta_2\right)}{\varphi\alpha_2\mathrm{P_{s1}}\Omega_{\mathrm{h}}}+\frac{2\left(\alpha_1+\alpha_2\right)}{\varphi\alpha_2\mathrm{P_{s2}}\Omega_{\mathrm{g}}}\right)^{-1}\mathrm{G}_{2,1}^{1,2}\left(\frac{\frac{\left((\beta_1+\beta_2)\varphi\alpha_2\mathrm{P_{s2}}\Omega_{\mathrm{g}}+(\alpha_1+\alpha_2)\varphi\alpha_2\mathrm{P_{s1}}\Omega_{\mathrm{h}}\right)\mathrm{P_{s2}}\Omega_{\mathrm{c}}}{\varphi^2\alpha_2^2\mathrm{P_{s1}}\Omega_{\mathrm{h}}\mathrm{P_{s2}}\Omega_{\mathrm{g}}}}{\left(\frac{2\varphi+2(\beta_1+\beta_2)}{\varphi\alpha_2\mathrm{P_{s1}}\Omega_{\mathrm{h}}}+\frac{2(\alpha_1+\alpha_2)}{\varphi\alpha_2\mathrm{P_{s2}}\Omega_{\mathrm{g}}}\right)}\middle|\begin{matrix}0,0\\0,-\end{matrix}\right)$$
$$+B_5\left(\frac{2\varphi+2\left(\beta_1+\beta_2\right)}{\varphi\alpha_2P_{s1}\Omega_h}+\frac{2\left(\alpha_1+\alpha_2\right)}{\varphi\alpha_2P_{s2}\Omega_g}\right)^{-1}G_{2,1}^{1,2}\left(\frac{\frac{P_r\Omega_b}{\alpha_2P_{s1}\Omega_h}}{\left(\frac{2\varphi+2(\beta_1+\beta_2)}{\varphi\alpha_2P_{s1}\Omega_h}+\frac{2(\alpha_1+\alpha_2)}{\varphi\alpha_2P_{s2}\Omega_g}\right)}\middle|\begin{matrix}0,0\\0,-\end{matrix}\right)$$
$$+B_6\left(\frac{2\varphi+2\left(\beta_1+\beta_2\right)}{\varphi\alpha_2P_{s1}\Omega_h}+\frac{2\left(\alpha_1+\alpha_2\right)}{\varphi\alpha_2P_{s2}\Omega_g}\right)^{-1}G_{2,1}^{1,2}\left(\frac{1}{\left(\frac{2\varphi+2(\beta_1+\beta_2)}{\varphi\alpha_2P_{s1}\Omega_h}+\frac{2(\alpha_1+\alpha_2)}{\varphi\alpha_2P_{s2}\Omega_g}\right)}\middle|\begin{matrix}0,0\\0,-\end{matrix}\right). \tag{24}$$

Proof. See Appendix C. □

D. Throughput Analysis

The throughput analysis of the two-way relay network is investigated in this subsection. First, utilizing the CDF-based throughput performance metric, [47, Eq. (15(*a*))], the throughput of x_1, x_2, y_1, and y_2 can be formulated as:

$$\tau_{x_i,y_i}^{\mathrm{up}} = \gamma_{th}\left(1-F_{x_i,y_i}^{\mathrm{up}}(\gamma_{th})\right), \forall_i = 1,2. \tag{25}$$

Substituting the related CDF expressions, which are (15), (16), (17), and (18), into (25), the analytical throughput expressions can be obtained. The aforementioned analytical expressions are omitted for brevity.

E. Asymptotic Analysis

In an effort to provide further insight of the derived analytical results, this subsection focuses on the high SNR regimes.

1) Outage Probability: By using the Taylor series expansion, the exp(x) term can be approximated to $1+x$, $x \longrightarrow 0$ [43]. By performing this variable change, the following expressions can be obtained.

$$F_{\gamma_{y_1}}^{\mathrm{S_1up}(\infty)}(\gamma_{\mathrm{th}}) = 1 - \left(1 - \gamma_{\mathrm{th}}\left(\frac{2(\beta_1+\beta_2)}{\varphi\beta_1 P_{s1}\Omega_h} + \frac{2\varphi + 2(\alpha_1+\alpha_2)}{\varphi(\beta_1 - \gamma_{th}\beta_2) P_{s2}\Omega_g}\right)\right) \times \frac{1}{P_{s1}\Omega_a}\left(\frac{(\beta_1+\beta_2)\gamma_{\mathrm{th}}}{\varphi\beta_1 P_{s1}\Omega_h} + \frac{(\alpha_1+\alpha_2)\gamma_{\mathrm{th}}}{\varphi(\beta_1 - \gamma_{th}\beta_2) P_{s2}\Omega_g} + \frac{1}{P_{s1}\Omega_a}\right)^{-1} \frac{1}{P_r\Omega_b}\left(\frac{\gamma_{\mathrm{th}}}{(\beta_1 - \gamma_{th}\beta_2) P_{s2}\Omega_g} + \frac{1}{P_r\Omega_b}\right)^{-1}, \tag{26}$$

$$F_{\gamma_{y_2}}^{\mathrm{S_1up}(\infty)}(\gamma_{\mathrm{th}}) = 1 - \left(1 - \gamma_{\mathrm{th}}\left(\frac{2(\beta_1+\beta_2)}{\varphi\beta_2 P_{s1}\Omega_h} + \frac{2\varphi + 2(\alpha_1+\alpha_2)}{\varphi\beta_2 P_{s2}\Omega_g}\right)\right) \times \frac{1}{P_{s1}\Omega_a}\left(\frac{(\beta_1+\beta_2)\gamma_{\mathrm{th}}}{\varphi\beta_2 P_{s1}\Omega_h} + \frac{(\alpha_1+\alpha_2)\gamma_{\mathrm{th}}}{\varphi\beta_2 P_{s2}\Omega_g} + \frac{1}{P_{s1}\Omega_a}\right)^{-1} \frac{1}{P_r\Omega_b}\left(\frac{\gamma_{\mathrm{th}}}{\beta_2 P_{s2}\Omega_g} + \frac{1}{P_r\Omega_b}\right)^{-1}, \tag{27}$$

$$F_{\gamma_{x_1}}^{\mathrm{S_2up}(\infty)}(\gamma_{\mathrm{th}}) = 1 - \left(1 - \gamma_{\mathrm{th}}\left(\frac{2\varphi + 2(\beta_1+\beta_2)}{\varphi(\alpha_1 - \gamma_{th}\alpha_2) P_{s1}\Omega_h} + \frac{2(\alpha_1+\alpha_2)}{\varphi\alpha_1 P_{s2}\Omega_g}\right)\right) \times \frac{1}{P_{s2}\Omega_c}\left(\frac{\gamma_{\mathrm{th}}(\beta_1+\beta_2)}{\varphi(\alpha_1 - \gamma_{th}\alpha_2) P_{s1}\Omega_h} + \frac{(\alpha_1+\alpha_2)\gamma_{\mathrm{th}}}{\varphi\alpha_1 P_{s2}\Omega_g} + \frac{1}{P_{s2}\Omega_c}\right)^{-1} \frac{1}{P_r\Omega_b}\left(\frac{\gamma_{\mathrm{th}}}{(\alpha_1 - \gamma_{th}\alpha_2) P_{s1}\Omega_h} + \frac{1}{P_r\Omega_b}\right)^{-1}, \tag{28}$$

$$F_{\gamma_{x_2}}^{\mathrm{S_2up}(\infty)}(\gamma_{\mathrm{th}}) = 1 - \left(1 - \gamma_{\mathrm{th}}\left(\frac{2\varphi + 2(\beta_1+\beta_2)}{\varphi\alpha_2 P_{s1}\Omega_h} + \frac{2(\alpha_1+\alpha_2)}{\varphi\alpha_2 P_{s2}\Omega_g}\right)\right) \times \frac{1}{P_{s2}\Omega_c}\left(\frac{(\beta_1+\beta_2)\gamma_{\mathrm{th}}}{\varphi\alpha_2 P_{s1}\Omega_h} + \frac{(\alpha_1+\alpha_2)\gamma_{\mathrm{th}}}{\varphi\alpha_2 P_{s2}\Omega_g} + \frac{1}{P_{s2}\Omega_c}\right)^{-1} \frac{1}{P_r\Omega_b}\left(\frac{\gamma_{\mathrm{th}}}{\alpha_2 P_{s1}\Omega_h} + \frac{1}{P_r\Omega_b}\right)^{-1}. \tag{29}$$

2) Ergodic Rate: Regarding the asymptotic derivations of $ER_{\gamma_{y_2}}^{\mathrm{S_1up}}$, utilizing [48, Eq. (07.34.03.0392.01)], the first part of $ER_{\gamma_{y_2}}^{\mathrm{S_1up}}$ can be written as:

$$B_1\xi^{-1}G_{2,1}^{1,2}\left(\frac{\theta}{\xi}\middle|\begin{matrix}0,0\\0,-\end{matrix}\right) = \mathrm{B_1}\xi^{-1}\left(\frac{\theta}{\xi}\right)^{-1}\mathrm{U}\left(1,1,\frac{\xi}{\theta}\right), \tag{30}$$

where $\xi = \left(\frac{2(\beta_1+\beta_2)}{\varphi\beta_2 P_{s1}\Omega_h} + \frac{2\varphi+2(\alpha_1+\alpha_2)}{\varphi\beta_2 P_{s2}\Omega_g}\right)$ and $\theta = \frac{\left((\beta_1+\beta_2)\varphi\beta_2 P_{s2}\Omega_g + (\alpha_1+\alpha_2)\varphi\beta_2 P_{s1}\Omega_h\right)P_{s1}\Omega_a}{\varphi^2\beta_2^2 P_{s1}\Omega_h P_{s2}\Omega_g}$.
Utilizing [49, Eq. (07.33.06.0012.01)], (30) can be written as

$$\mathrm{B_1}\xi^{-1}\left(1 + \mathrm{O}\left(\frac{\theta}{\xi}\right)\right), \tag{31}$$

where O represents the higher order term. Following a similar procedure, the other parts of $ER_{\gamma_{y_2}}^{\mathrm{S_1up}}$ and $ER_{\gamma_{x_2}}^{\mathrm{S_2up}}$ can be obtained. These derivations are omitted for brevity. Regarding the asymptotic expressions of $ER_{\gamma_{y_1}}^{\mathrm{S_1up}}$ and $ER_{\gamma_{x_1}}^{\mathrm{S_2up}}$, utilizing $\exp(\mathrm{x}) \approx 1+\mathrm{x}$, $x \longrightarrow 0$ [43] and substituting into (51) and (52), the asymptotic integral expressions can be obtained.

IV. Optimization

This section presents the transmit power and power allocation coefficients optimization under fixed relay position, and optimized relay position when fixed resource allocation is considered.

A. Resource Allocation Optimization under Fixed Relay Location

The optimization problem of minimizing the outage probabilities of S_1 and S_2 and its constraints can be written as:

$$\begin{aligned} \underset{\gamma_{th}}{\text{minimize}} \quad & \mathrm{F}^{\mathrm{S_1up}\infty}_{\gamma_{\mathrm{y}_1}}(\gamma_{\mathrm{th}}), \mathrm{F}^{\mathrm{S_1up}\infty}_{\gamma_{\mathrm{y}_2}}(\gamma_{\mathrm{th}}) \\ & \text{and } \mathrm{F}^{\mathrm{S_2up}\infty}_{\gamma_{\mathrm{x}_1}}(\gamma_{\mathrm{th}}), \mathrm{F}^{\mathrm{S_2up}\infty}_{\gamma_{\mathrm{x}_2}}(\gamma_{\mathrm{th}}) \\ \text{subject to} \quad & 2P_s + P_r = P \text{ and } 0 < P_s, P_r \text{ and } P_{s1} = P_{s2} = P_s, \\ \text{subject to} \quad & \alpha_1 + \alpha_2 = 1, \beta_1 + \beta_2 = 1 \text{ and } \alpha_1 > \alpha_2, \beta_1 > \beta_2. \end{aligned} \tag{32}$$

We define $a_2 = \frac{\gamma_{th}}{\Omega_h}$ and $b_2 = \frac{\gamma_{th}}{\Omega_g}$ and also $P_{s1} = p_{fs1}P$, $P_{s2} = p_{fs2}P$, $P_r = \left(1 - p_{fs1} - p_{fs2}\right)P$, $p_{fs1}, p_{fs2} \epsilon\, (0,1)$, $p_{fs1} = \alpha_1 + \alpha_2$, $p_{fs2} = \beta_1 + \beta_2$. Substituting p_f into P_s and P_r, the transmit power levels are obtained as: $P_{s1} = (\alpha_1 + \alpha_2)\, P$, $P_{s2} = (\beta_1 + \beta_2)\, P$, $P_r = (1 - \beta_1 - \beta_2 - \alpha_1 - \alpha_2)\, P$, where $0 < \beta_2 < \beta_1 < 1$, $0 < \alpha_2 < \alpha_1 < 1$ and $P > 0$. By performing these variable changes, $F^{\mathrm{up}\infty}_{\gamma\mathrm{x}_1}(\gamma_{\mathrm{th}})$, (12) and $F^{\mathrm{up}\infty}_{\gamma\mathrm{x}_2}(\gamma_{\mathrm{th}})$, (13) can be re-written as:

$$\begin{aligned} F^{\mathrm{S_1up}(\infty)}_{\gamma_{\mathrm{y}_1}}(\gamma_{\mathrm{th}}) &= 1 - \left(1 - \left(\frac{2a_2\,(\beta_1+\beta_2)}{\varphi\beta_1\,(\alpha_1+\alpha_2)\,P} + \frac{(2\varphi + 2\,(\alpha_1+\alpha_2))\,b_2}{\varphi\,(\beta_2 - \gamma_{th}\beta_1)\,(\beta_1+\beta_2)\,P}\right)\right) \\ &\quad \times \left(\frac{a_2\,(\beta_1+\beta_2)\,\Omega_a}{\varphi\beta_1} + \frac{b_2\,(\alpha_1+\alpha_2)^2\,\Omega_a}{\varphi\,(\beta_1 - \gamma_{th}\beta_2)\,(\beta_1+\beta_2)} + 1\right)^{-1} \left(\frac{b_2\Omega_b\,(1-\beta_1-\beta_2-\alpha_1-\alpha_2)}{(\beta_1 - \gamma_{th}\beta_2)\,(\beta_1+\beta_2)} + 1\right)^{-1}, \end{aligned} \tag{33}$$

$$\begin{aligned} F^{\mathrm{S_1up}(\infty)}_{\gamma_{\mathrm{y}_2}}(\gamma_{\mathrm{th}}) &= 1 - \left(1 - \gamma_{th}\left(\frac{2a_2\,(\beta_1+\beta_2)}{\varphi\beta_2\,(\alpha_1+\alpha_2)\,P} + \frac{(2\varphi + 2\,(\alpha_1+\alpha_2))\,b_2}{\varphi\beta_2\,(\beta_1+\beta_2)\,P}\right)\right) \\ &\quad \times \left(\frac{(\beta_1+\beta_2)\,\Omega_a a_2}{\varphi\beta_2} + \frac{(\alpha_1+\alpha_2)^2\,\Omega_a b_2}{\varphi\beta_2\,(\beta_1+\beta_2)} + 1\right)^{-1} \left(\frac{b_2\Omega_b\,(1-\beta_1-\beta_2-\alpha_1-\alpha_2)}{\beta_2\,(\beta_1+\beta_2)} + 1\right)^{-1}, \end{aligned} \tag{34}$$

$$\begin{aligned} F^{\mathrm{S_2up}(\infty)}_{\gamma_{\mathrm{x}_1}}(\gamma_{\mathrm{th}}) &= 1 - \left(1 - \left(\frac{(2\varphi + 2\,(\beta_1+\beta_2))\,a_2}{\varphi\,(\alpha_1 - \gamma_{th}\alpha_2)\,(\alpha_1+\alpha_2)\,P} + \frac{2b_2\,(\alpha_1+\alpha_2)}{\varphi\alpha_1\,(\beta_1+\beta_2)\,P}\right)\right) \\ &\quad \times \left(\frac{a_2\Omega_c\,(\beta_1+\beta_2)^2}{\varphi\,(\alpha_1 - \gamma_{th}\alpha_2)\,(\alpha_1+\alpha_2)} + \frac{b_2\Omega_c\,(\alpha_1+\alpha_2)}{\varphi\alpha_1} + 1\right)^{-1} \left(\frac{a_2\Omega_b\,(1-\beta_1-\beta_2-\alpha_1-\alpha_2)}{(\alpha_1 - \gamma_{th}\alpha_2)\,(\alpha_1+\alpha_2)} + 1\right)^{-1}, \end{aligned} \tag{35}$$

$$\begin{aligned} F^{\mathrm{S_2up}(\infty)}_{\gamma_{\mathrm{x}_2}}(\gamma_{\mathrm{th}}) &= 1 - \left(1 - \left(\frac{(2\varphi + 2\,(\beta_1+\beta_2))\,a_2}{\varphi\alpha_2\,(\alpha_1+\alpha_2)\,P} + \frac{2b_2\,(\alpha_1+\alpha_2)}{\varphi\alpha_2\,(\beta_1+\beta_2)\,P}\right)\right) \\ &\quad \times \left(\frac{a_2\,(\beta_1+\beta_2)^2\,\Omega_c}{\varphi\alpha_2\,(\alpha_1+\alpha_2)} + \frac{b_2\Omega_c\,(\alpha_1+\alpha_2)}{\varphi\alpha_2} + 1\right)^{-1} \left(\frac{a_2\Omega_b\,(1-\beta_1-\beta_2-\alpha_1-\alpha_2)}{\alpha_2\,(\alpha_1+\alpha_2)} + 1\right)^{-1}. \end{aligned} \tag{36}$$

By using the Lagrangian multiplier and considering the first term of $F^{\mathrm{S_1up}(\infty)}_{\gamma_{\mathrm{y}_1}}(\gamma_{\mathrm{th}})$, differentiation with respect to β_1 and β_2 and also, setting the obtained result to zero, the following expressions can be obtained.

$$\frac{\partial \mathcal{L}\left(F_{\gamma_{y_1}}^{S_1 up(\infty)}(\gamma_{th})\right)}{\partial \beta_1} = (2a_2)\left(\varphi\beta_1(\alpha_1+\alpha_2)P\right)^{-1} + (2a_2)(\beta_1+\beta_2)\left(\varphi\beta_1(\alpha_1+\alpha_2)P\right)^{-2}(\varphi(\alpha_1+\alpha_2)P) + (\varphi(\beta_2-\gamma_{th}\beta_1)(\beta_1+\beta_2)P)^{-1} + ((2\varphi+2(\alpha_1+\alpha_2))b_2)(\varphi(\beta_2-\gamma_{th}\beta_1)(\beta_1+\beta_2)P)^{-2} \times (\varphi\beta_2 P - 2\varphi\gamma_{th}\beta_1 - \varphi\gamma_{th}\beta_2 P), \quad (37)$$

$$\frac{\partial \mathcal{L}\left(F_{\gamma_{y_1}}^{S_1 up(\infty)}(\gamma_{th})\right)}{\partial \beta_2} = (2a_2)\left(\varphi\beta_1(\alpha_1+\alpha_2)P\right)^{-1} + ((2\varphi+2(\alpha_1+\alpha_2))b_2)(\varphi(\beta_2-\gamma_{th}\beta_1)(\beta_1+\beta_2)P)^{-2} \times (\varphi\beta_1 P + 2\varphi\beta_2 P - \varphi\gamma_{th}\beta_1 P). \quad (38)$$

Utilizing $2\varphi\gamma_{th}\beta_1 - \varphi\gamma_{th}\beta_2 P$ in (37) and setting to zero and also taking into consideration the constraint in (34), β_1 and β_2 are found to be equal to $\frac{1}{3}$ and $\frac{2}{3}$, respectively. However, the obtained result is not consistent with the order of power allocation coefficients, which is $\beta_2 < \beta_1$. Therefore, utilizing $\varphi\beta_1 P + 2\varphi\beta_2 P$ in (37) and setting to zero, β_1 and β_2 are equal to $\frac{2}{3}$ and $\frac{1}{3}$, respectively.

Likewise, following a similar procedure, by using the Lagrangian multiplier and considering the first term of $F_{\gamma_{x_1}}^{S_2 up(\infty)}(\gamma_{th})$, and also differentiation with respect to α_1, α_2 and setting the obtained result to zero, the following expressions can be obtained.

$$\frac{\partial \mathcal{L}\left(F_{\gamma_{x_1}}^{S_2 up(\infty)}(\gamma_{th})\right)}{\partial \alpha_1} = ((2\varphi+2(\beta_1+\beta_2))a_2)(\varphi(\alpha_1-\gamma_{th}\alpha_2)(\alpha_1+\alpha_2)P)^{-2} \times (2\varphi P\alpha_1 + \varphi\alpha_2 P - \varphi\gamma_{th}\alpha_2 P) + 2b_2(\varphi\alpha_1(\beta_1+\beta_2)P)^{-1} + 2b_2(\alpha_1+\alpha_2)(\varphi\alpha_1(\beta_1+\beta_2)P)^{-2}(\varphi(\beta_1+\beta_2)P), \quad (39)$$

$$\frac{\partial \mathcal{L}\left(F_{\gamma_{x_1}}^{S_2 up(\infty)}(\gamma_{th})\right)}{\partial \alpha_2} = ((2\varphi+2(\beta_1+\beta_2))a_2)(\varphi(\alpha_1-\gamma_{th}\alpha_2)(\alpha_1+\alpha_2)P)^{-2} \times (\varphi P\alpha_1 - \varphi\alpha_1\gamma_{th}P - 2\varphi\gamma_{th}\alpha_2 P) + 2b_2(\varphi\alpha_1(\beta_1+\beta_2)P)^{-1}. \quad (40)$$

Utilizing $2\varphi P\alpha_1 + \varphi\alpha_2 P$ in (39) and setting to zero and also taking into consideration the constraint in (32), α_1 and α_2 are found to be equal to $\frac{1}{3}$ and $\frac{2}{3}$, respectively. Again, the obtained result is not consistent with the order of power allocation coefficients, which is $\alpha_2 < \alpha_1$. Therefore, utilizing $\varphi\gamma_{th}\alpha_1 P - 2\gamma_{th}\varphi\alpha_2 P$ in (40) and setting to zero, α_1 and α_2 are equal to $\frac{2}{3}$ and $\frac{1}{3}$, respectively.

Next, the transmit power optimization procedure is presented. As shown in (32), S_1, S_2, and the relay terminal have transmit power denoted as P_{s1}=P_{s2}=P and P_r. As such, the total transmit power of the system is equal to

$2P_s + P_r = P$. Thus, the relay's transmit power can be re-written as: $P_r = P - 2P_s$. Substituting the newly obtained relay's transmit power into the asymptotic CDF expression and differentiating with respect to P_s, the following result can be obtained

$$\begin{aligned}\frac{\partial \mathcal{L}\left(F_{\gamma_{y_1}}^{\mathrm{S_1up}(\infty)}(\gamma_{\mathrm{th}})\right)}{\partial P_s} &= (P-2P_s)\,P_s^{-1} \\ &= -2P_s^{-1} - (P-2P_s)\,P_s^{-2}. \end{aligned} \tag{41}$$

Setting the obtained result to zero, S_1 and S_2's optimal transmit powers, denoted as P_s^*, can be obtained as $\frac{P}{4}$. Finally, the relay's optimal transmit power, P_r^*, is equal to $\frac{P}{2}$.

B. Relay Position Optimization under Fixed Resource Allocation

Here, the optimization of the relay location for two-way communication is presented. By means of Euclidean distance formulation, the path-losses between $S_1 \rightarrow$ relay and relay $\rightarrow S_2$are denoted as d^v and $(1-d)^v$, respectively. The d term represents the distance and v term represents the path-loss exponent. Therefore, Ω_h and Ω_g can be written as: $\frac{1}{d^v}$ and $\frac{1}{(1-d)^v}$, respectively. By performing the variable change in $F_{\gamma_{y_1}}^{\mathrm{S_1up}(\infty)}(\gamma_{\mathrm{th}})$, (33), the following results can be obtained.

$$\begin{aligned}F_{\gamma_{y_1}}^{\mathrm{S_1up}(\infty)}(\gamma_{\mathrm{th}}) &= 1 - (1 - (A_1 d^v + A_2\,(1-d)^v)) \\ &\quad \times (A_3 d^v + A_4\,(1-d)^v + 1)^{-1}\,(A_5\,(1-d)^v + 1)^{-1}, \end{aligned} \tag{42}$$

where $A_1 = \gamma_{\mathrm{th}}\left(\frac{2(\beta_1+\beta_2)}{\varphi\beta_1 P_{s1}}\right)$, $A_2 = \gamma_{\mathrm{th}}\left(\frac{2\varphi+2(\alpha_1+\alpha_2)}{\varphi(\beta_1-\gamma_{th}\beta_2)P_{s2}}\right)$, $A_3 = \left(\frac{\Omega_a(\beta_1+\beta_2)\gamma_{\mathrm{th}}}{\varphi\beta_1}\right)$, $A_4 = \left(\frac{P_{s1}\Omega_a(\alpha_1+\alpha_2)\gamma_{\mathrm{th}}}{\varphi(\beta_1-\gamma_{th}\beta_2)P_{s2}}\right)$, $A_5 = \left(\frac{P_r\Omega_b\gamma_{\mathrm{th}}}{(\beta_1-\gamma_{th}\beta_2)P_{s2}}\right)$. Differentiating (42) with respect to d, the following results can be obtained.

$$\begin{aligned}\frac{\partial \mathcal{L}\left(F_{\gamma_{y_1}}^{\mathrm{S_1up}(\infty)}(\gamma_{\mathrm{th}})\right)}{\partial d} &= \left(A_1 v d^{v-1} + A_2\left(v\,(1-d)^{v-1}\right)\right) \\ &\quad \times (A_3 d^v + A_4\,(1-d)^v + 1)^{-2} \\ &\quad \times \left(A_3 v d^{v-1} + A_4 v\,(1-d)^{v-1}\right) \\ &\quad \times (A_5\,(1-d)^v + 1)^{-2}\left(A_5 v\,(1-d)^{v-1}\right) \\ &\quad \Longrightarrow \left(v d^{v-1} + v(1-d)^{v-1}\right) = 0 \Longrightarrow d = \frac{1}{2}. \end{aligned} \tag{43}$$

V. Numerical Results

The results of the theoretical analysis are evaluated and validated by means of Monte-Carlo simulations. In order to obtain the numerical results, based on the expressions that were derived in Section 3, we have used Matlab®. Also, in order to evaluate Meijer's G function, we have used the Symbolic Math Toolbox. Two different cases, i.e. non-optimized and optimized, are considered in this section. In the non-optimized, the power allocation coefficients, α_1, α_2, and β_1, β_2, are set to $9/10$, $1/10$ and $9/10$, $1/10$, respectively. Regarding the non-optimized transmit powers, equal power allocation is assumed for all the terminals in the network,i.e. $P/3$. In the optimized case, following the results of the optimization procedure, the power allocation coefficients α_1, α_2, and β_1, β_2, are set to $2/3$, $1/3$ and

2/3, 1/3, respectively. As for the non-optimized transmit power allocation, each user employs $P/4$ transmit power, while the relay terminal uses $P/2$ transmit power. The LI variances, σ_a^2, σ_b^2, and σ_c^2 are modeled as: $\sigma_a^2 P_{s1}^{\lambda-1}$, $\sigma_b^2 P_r^{\lambda-1}$, and $\sigma_c^2 P_{s2}^{\lambda-1}$ [50, Eq. (8)]. The λ parameter takes values $0 \leq \lambda \leq 1$ [50, Eq. (8)] and specifically, $\lambda = 0.2$ is considered. According to the optimization section, the relay terminal is located halfway of the user terminals. Note that as (7), (8), (9), and (10) have intractable forms, these expressions are upper-bounded using $\frac{\mathrm{AB}}{\mathrm{A+B}} \leq \min(\mathrm{A}, \mathrm{B})$. In this regard, the obtained analytical derivations are upper-bounded. For this reason, a small gap is observed between simulations, analytical, and asymptotic results.

Figure 2 presents the optimized and non-optimized outage performance comparison of x_1 and x_2 at S_2. The obtained results reveal that power allocation coefficients and transmit power optimization leads to equal outage performance for x_1 and x_2. As an example, to reach 10^{-3} outage level, the required SNRs are roughly between 40-45 dB and 50 dB for the non-optimized x_1 and x_2, respectively. To achieve the same outage level with the optimized case, the required SNR is between 44-46 dB for x_1 and x_2. On the contrary, for the non-optimized case, it is observed that x_1 has significantly worst outage performance, compared to x_2, threatening the communication reliability.

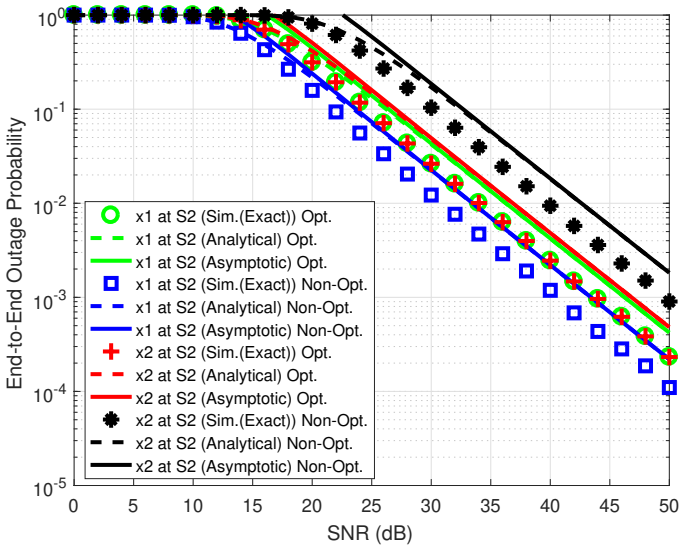

Fig. 2: Optimized and non-optimized outage performance comparison of x_1 and x_2 at S_2.

Figure 3 presents the optimized and non-optimized outage probability performance comparison of y_1 and y_2 at S_1. As it is the case in figure 2, power allocation coefficients and transmit power optimization provide an equal outage performance for y_1 and y_2 at S_2. The obtained results are found closely in an agreement with the derived analytical and asymptotic results, in (26), (27) and (33), (34).

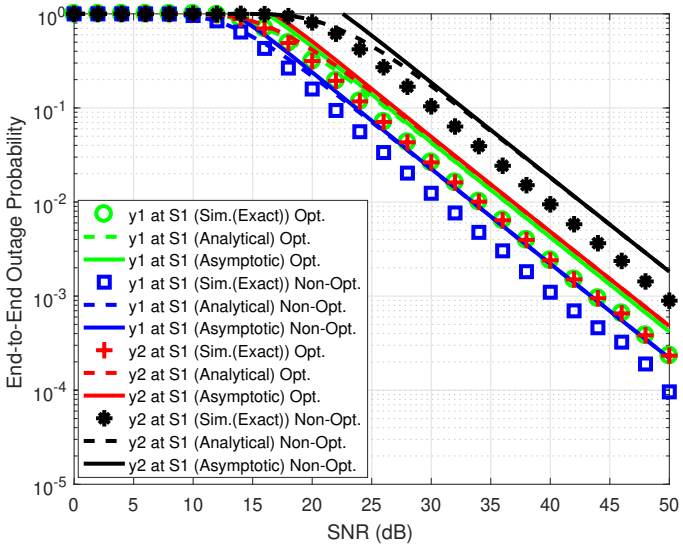

Fig. 3: Optimized and non-optimized outage performance comparison of y_1 and y_2 at S_1.

Figure 4 presents the optimized and non-optimized throughput performance comparison of x_1 and x_2 at S_2. As it was shown in figures 2 and 3, power allocation coefficients and transmit power optimization result in an equal throughput performance for x_1 and x_2 at S_1. It can be seen that in order to achieve 0.7 bps/Hz throughput performance, the required SNR values are 20 dB and between 25-30 dB for x_1 and x_2, respectively, in the non-optimized case. However, in the optimized case, the curves for x_1 and x_2 coincide at 20 dB for 0.7 bps/Hz throughput performance.

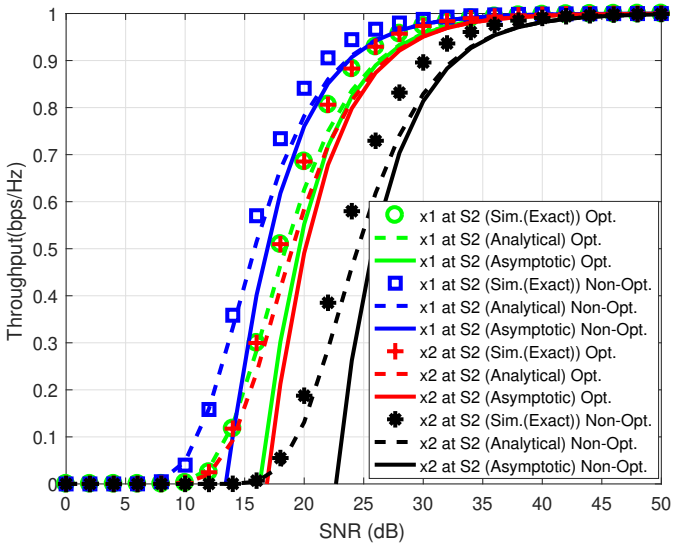

Fig. 4: Optimized and non-optimized throughput performance comparison of x_1 and x_2 at S_2.

Figure 5 presents the optimized and non-optimized throughput performance comparison of y_1 and y_2 at S_1. Like in figure 4, the optimized power allocation coefficients and transmit power provide an equal throughput performance for y_1 and y_2 at S_2. The obtained results closely match the derived analytical and asymptotic results.

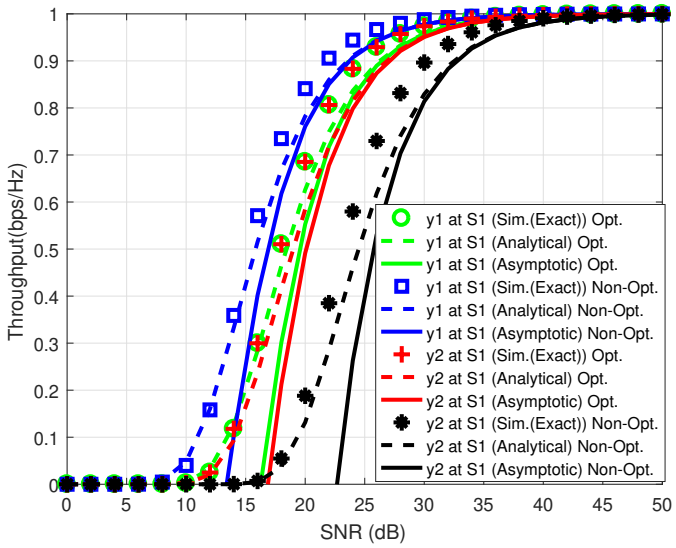

Fig. 5: Optimized and non-optimized throughput performance comparison of y_1 and y_2 at S_1.

Figure 6 plots the optimized and non-optimized EP performance comparison of x_1 and x_2 at S_2. The optimized x_2 achieves a better performance than non-optimized x_2. This is because, in the non-optimized case, the power allocation coefficient is $1/9$ while it is $1/3$ in optimized case. For instance, to achieve 10^{-3} EP performance, the optimized and non-optimized x_2 require 38 dB and 44 dB, respectively. Regarding the EP performance of x_1, the non-optimized case achieves a better performance than its counterpart optimized case. This is because, the non-optimized case has $9/10$ power allocation coefficients while optimized case has $2/3$. The aforementioned differences cause system coding gain gap and an error floor for the optimized x_1 after 25 dB. However, up to that point an almost identical performance for x_1 and x_2 is observed, contrary to the non-optimized curves.

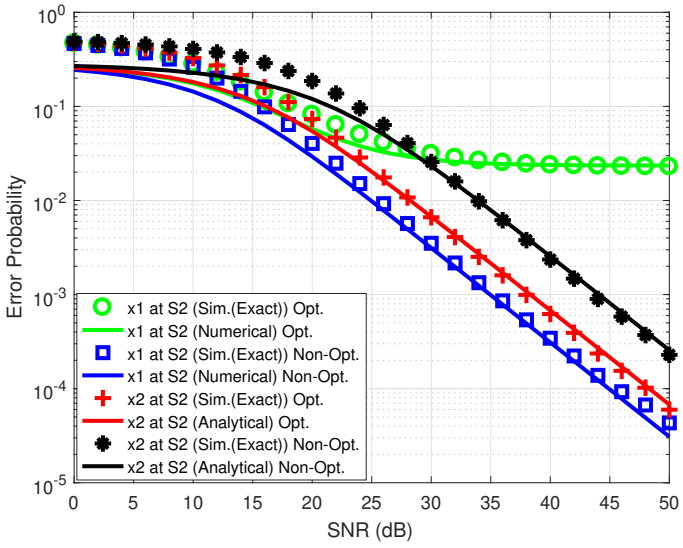

Fig. 6: Optimized and non-optimized EP performance comparison of x_1 and x_2 at S_2.

Figure 7 plots the optimized and non-optimized EP performance comparison of y_1 and y_2 at S_1. Like in figure 6, the optimized power allocation coefficients and transmit powers provide a better EP performance for y_2 at S_1.

However, the non-optimized y_1 achieves a better EP performance than its counterpart in the optimize case. Again, this behaviour results from the power allocation coefficient differences. Still, a homogeneous performance among x_1 and x_2 can be seen until 25 dB in the optimized case. The obtained results are in close agreement with the derived analytical and numerical results, in (20) and (21).

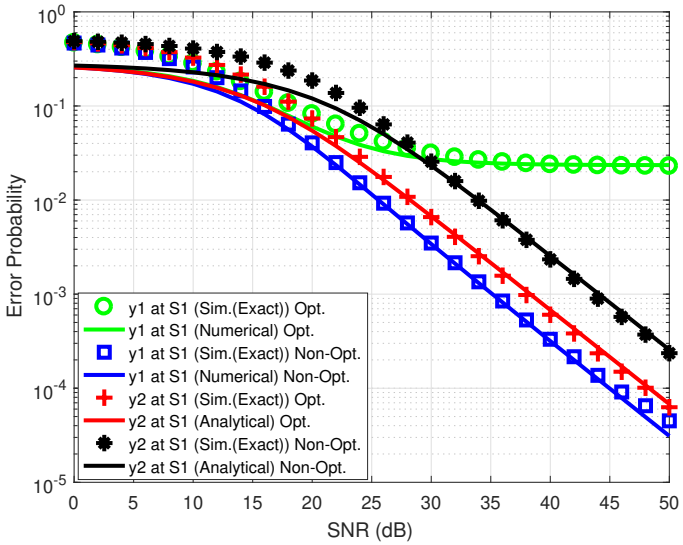

Fig. 7: Optimized and non-optimized EP performance comparison of y_1 and y_2 at S_1.

Figure 8 plots the ER performance comparison of x_1 and x_2 at S_2. According to figure 8, the non-optimized x_1 provides a better ER performance than its optimized counterpart. This performance gap occurs because in the non-optimized case the power allocation coefficient takes a value of $9/10$ while in the optimized case it is equal to $2/3$. In the high SNR regime, the optimized and non-optimized x_1 saturate and cause system coding gain losses. This error floor is a result of the detrimental effects of LI. Regarding the performance of x_2, the optimized case achieves a better ER performance than its non-optimized counterpart. The aforementioned difference occurs due to the power allocation coefficients differences between the two cases.

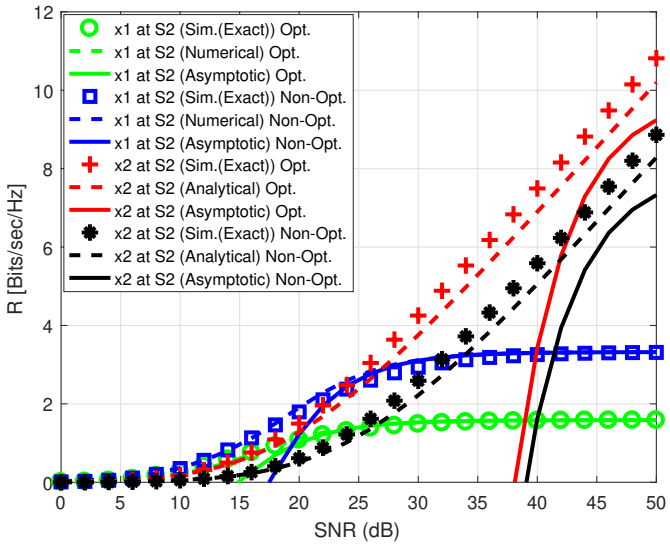

Fig. 8: Optimized and non-optimized ER performance comparison of x_1 and x_2 at S_2.

Figure 9 presents the ER performance comparison of y_1 and y_2 at S_1. Like in figure 8, the optimized power allocation coefficients and transmit power provide a better ER performance for y_2 at S_1. On the other hand, the non-optimized y_1 achieves a better performance than that of the optimized case, as the non-optimized power allocation coefficient guarantees higher ER. The obtained results closely match the derived analytical and asymptotic results, in (23) and (24).

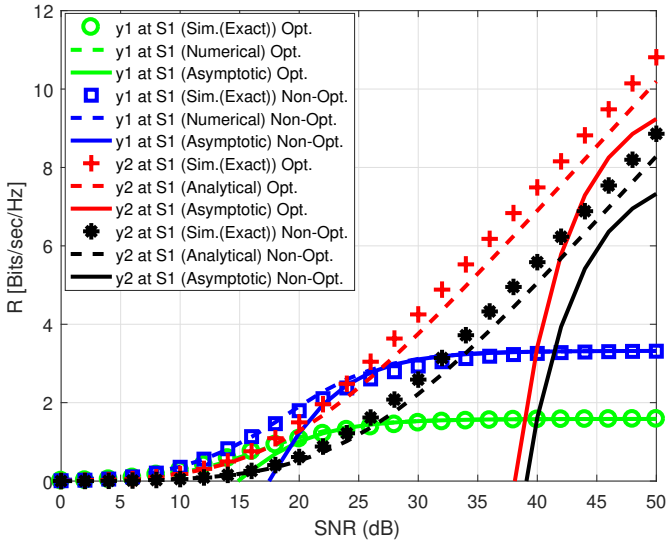

Fig. 9: Optimized and non-optimized ER performance comparison of y_1 and y_2 at S_1.

Figure 10 plots the OP performance versus the normalized distance for x_1 and x_2 at S_2. The SNR is set to 30 dB for the aforementioned analysis. It is observed that the OP of optimized and non-optimized x_1 reduces until the distance reaches values between 0.3-0.4. Then, the outage performance for the optimized and non-optimized cases deteriorates beyond this point. The non-optimized x_1 achieves a better outage performance than the optimized x_1. This behavior occurs due to the power allocation difference. The outage performance of the optimized and

non-optimized x_2 improves until the distance reaches values between 0.3-0.5 while for larger values, performance degradation is shown. The optimized x_2 provides a better outage performance than its non-optimized counterpart for the same distance due to power allocation differences. It must be noted that the proposed optimization reduces the outage performance gap among the two signals, contrary to the non-optimized case.

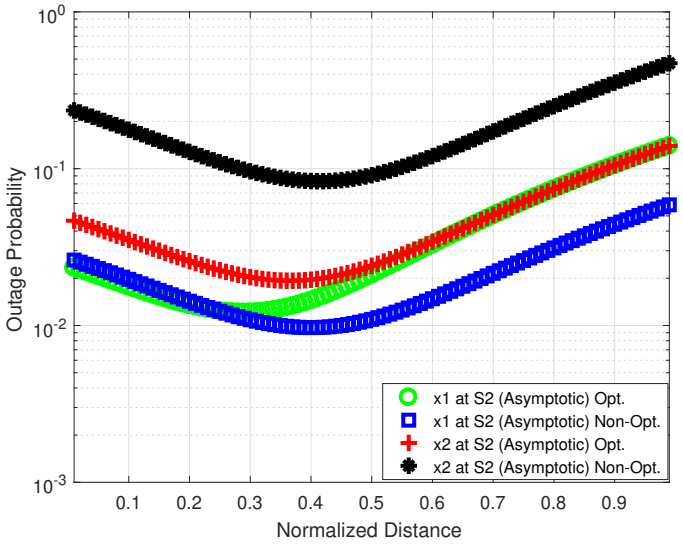

Fig. 10: OP versus normalized distance for x_1 and x_2 at S_2.

Figure 11 depicts the OP performance versus the normalized distance for y_1 and y_2 at S_1. When compared to the results depicted in figure 10, here, slightly different outage performance is observed. For instance, the outage performance of optimized and non-optimized y_1 improves until the distance reaches values between 0.5-0.7. Beyond this point, the outage performance deteriorates. The non-optimized y_1 achieves a better outage performance than that of the optimized case due to power allocation coefficient differences. Similarly, the outage performance of the optimized and non-optimized y_2 improves until the distance reaches values between 0.5-0.7 and after that point worse outage performance is obtained. Finally, the optimized y_2 achieves a better outage performance than the non-optimized y_2 but overall, the optimized case offers a more homogeneous outage performance for the two signals than the non-optimized case where a large performance gap can be seen.

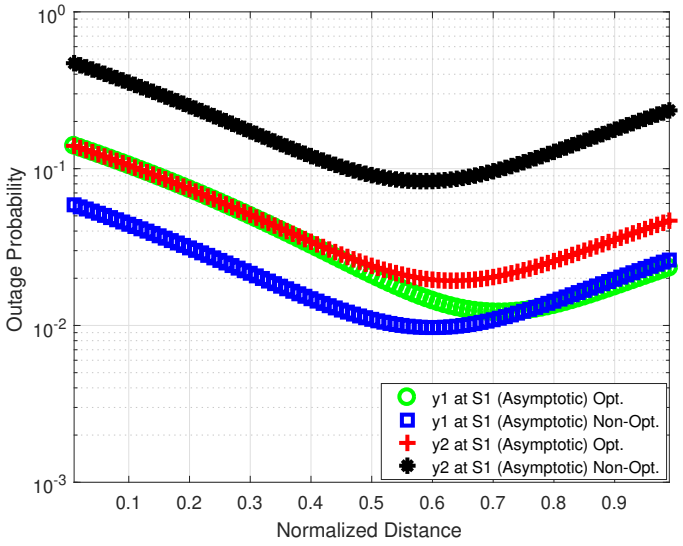

Fig. 11: OP versus normalized distance for y_1 and y_2 at S_1.

VI. Conclusions

This paper has investigated the performance of two-way relaying with non-orthogonal multiple access in the power-domain. A two-hop two-way amplify-and-forward relay network with full-duplex capabilities was considered where users exchanged superimposed signals and exploited echo-cancellation and successive interference cancellation to improve the reception quality. A thorough performance analysis was conducted, in terms of outage probability, error probability, ergodic rate and throughput and the network's performance was optimized by using the Lagrangian multiplier to obtain the optimal transmit power, power allocation coefficients and relay position. The analytical and asymptotic expressions were verified through Monte-Carlo simulations and results revealed that power allocation optimization plays a key role in enhancing the network performance.

Appendix

Since the variables are dependent to each other in (11), this paper follows section III of [44] and the following expressions can be obtained.

$$
\begin{aligned}
F_{\gamma_{y_1}}^{\mathrm{S_1up}}(\gamma_{\mathrm{th}}) &= P_r\left(\varphi\beta_1 \min(\mathrm{A},\mathrm{B}) \leq \underbrace{2^R-1}_{\gamma_{\mathrm{th}}}\right)\\
&= P_r\left(\min\left(\frac{\varphi\beta_1\gamma_{\mathrm{x}}}{(\gamma_{\mathrm{A}}(\beta_1+\beta_2)+(\beta_1+\beta_2))}, \frac{\varphi\beta_1\gamma_{\mathrm{y}}}{\left(\varphi\gamma_{\mathrm{y}}\beta_2+\varphi\gamma_{\mathrm{B}}+\gamma_{\mathrm{A}}(\alpha_1+\alpha_2)+\varphi+(\alpha_1+\alpha_2)\right)}\right) \leq \gamma_{\mathrm{th}}\right)\\
&= 1-P_r\left(\gamma_x \geq \frac{\gamma_{th}}{\varphi\beta_1}(\gamma_A(\beta_1+\beta_2)+(\beta_1+\beta_2)), \gamma_y \geq \frac{\gamma_{th}}{\varphi\beta_1}\left(\varphi\gamma_y\beta_2+\varphi\gamma_B+\gamma_A(\alpha_1+\alpha_2)+\varphi+(\alpha_1+\alpha_2)\right)\right)\\
&= 1-P_r\left(\gamma_x \geq \frac{\gamma_{th}}{\varphi\beta_1}(\gamma_a(\beta_1+\beta_2)+2(\beta_1+\beta_2)), \gamma_y \geq \frac{\gamma_{th}(\varphi\gamma_b+\gamma_a(\alpha_1+\alpha_2)+2\varphi+2(\alpha_1+\alpha_2))}{\varphi(\beta_1-\gamma_{th}\beta_2)}\right)\\
&= 1-\left(1-F_{\gamma_x}\left(\frac{\gamma_{th}}{\varphi\beta_1}(\gamma_a(\beta_1+\beta_2)+2(\beta_1+\beta_2))\right)\right.\\
&\times\left.\left(1-F_{\gamma_y}\left(\frac{\gamma_{th}(\varphi\gamma_b+\gamma_a(\alpha_1+\alpha_2)+2\varphi+2(\alpha_1+\alpha_2))}{\varphi(\beta_1-\gamma_{th}\beta_2)}\right)\right)\right.\\
&= 1-\mathbb{E}_{\gamma_a,\gamma_b}\left[e^{-\gamma_{\mathrm{th}}\left(\frac{(\gamma_a(\beta_1+\beta_2)+2(\beta_1+\beta_2))}{\varphi\beta_1 P_{s1}\Omega_h}+\frac{(\varphi\gamma_b+\gamma_a(\alpha_1+\alpha_2)+2\varphi+2(\alpha_1+\alpha_2))}{\varphi(\beta_1-\gamma_{th}\beta_2)P_{s2}\Omega_g}\right)}\Big|_{\gamma_a,\gamma_b}\right]\\
&= 1-e^{-\gamma_{\mathrm{th}}\left(\frac{2(\beta_1+\beta_2)}{\varphi\beta_1 P_{s1}\Omega_h}+\frac{2\varphi+2(\alpha_1+\alpha_2)}{\varphi(\beta_1-\gamma_{th}\beta_2)P_{s2}\Omega_g}\right)}\int_0^\infty e^{-\gamma_a\left(\frac{(\beta_1+\beta_2)\gamma_{\mathrm{th}}}{\varphi\beta_1 P_{s1}\Omega_h}+\frac{(\alpha_1+\alpha_2)\gamma_{\mathrm{th}}}{\varphi(\beta_1-\gamma_{th}\beta_2)P_{s2}\Omega_g}\right)} f_{\gamma_a}(\gamma_a)\,d\gamma_a\times\\
&\int_0^\infty e^{-\gamma_b\left(\frac{\gamma_{\mathrm{th}}}{(\beta_1-\gamma_{th}\beta_2)P_{s2}\Omega_g}\right)} f_{\gamma_b}(\gamma_b)\,d\gamma_b. \qquad (44)
\end{aligned}
$$

Substituting $f_{\gamma_a}(\gamma_a) = \frac{1}{P_{s1}\Omega_a}e^{-\frac{\gamma_a}{P_{s1}\Omega_a}}$ and $f_{\gamma_b}(\gamma_b) = \frac{1}{P_r\Omega_b}e^{-\frac{\gamma_b}{P_r\Omega_b}}$ [51], and solving the integral expressions with the help of [43, Eq. (3.310[11])], the final expression can be calculated as in (15). Following the same procedures, $F_{\gamma_{y_2}}^{\mathrm{S_1up}}(\gamma_{\mathrm{th}})$, $F_{\gamma_{x_1}}^{\mathrm{S_2up}}(\gamma_{\mathrm{th}})$, and $F_{\gamma_{x_2}}^{\mathrm{S_2up}}(\gamma_{\mathrm{th}})$ can be calculated as in (16), (17), and (18), respectively. Substituting (15) into (19) and using distributive properties, the following expression can be obtained.

$$
\begin{aligned}
\bar{P}_{e\,\gamma_{y_1}}^{\mathrm{S_1up}} = \frac{1}{2\sqrt{\pi}}\Bigg[&\int_0^\infty \gamma_{th}^{-\frac{1}{2}}\exp(-\gamma_{\mathrm{th}})\,\mathrm{d}\gamma_{\mathrm{th}} - \int_0^\infty \gamma_{\mathrm{th}}^{-\frac{1}{2}}\mathrm{e}^{-\gamma_{\mathrm{th}}\left(\frac{2(\beta_1+\beta_2)}{\varphi\beta_1\mathrm{P_{s1}}\Omega_{\mathrm{h}}}+\frac{2\varphi+2(\alpha_1+\alpha_2)}{\varphi(\beta_1-\gamma_{\mathrm{th}}\beta_2)\mathrm{P_{s2}}\Omega_{\mathrm{g}}}+1\right)}\\
&\times\left(\frac{1}{P_{s1}\Omega_a}\right)\left(\frac{(\beta_1+\beta_2)\gamma_{th}}{\varphi\beta_1 P_{s1}\Omega_h}+\frac{(\alpha_1+\alpha_2)\gamma_{th}}{\varphi(\beta_1-\gamma_{th}\beta_2)P_{s2}\Omega_g}+\frac{1}{P_{s1}\Omega_a}\right)^{-1}\\
&\times\left(\frac{1}{P_r\Omega_b}\right)\left(\frac{\varphi\gamma_{th}}{\varphi(\beta_1-\gamma_{th}\beta_2)P_{s2}\Omega_g}+\frac{1}{P_r\Omega_b}\right)^{-1}d\gamma_{th}\Bigg]. \qquad (45)
\end{aligned}
$$

With the help of [43, Eq. (3.326.2[10])], the first integral in (45) can be solved as $\Gamma\left(\frac{1}{2}\right)=\sqrt{\pi}$. Since the second integral has an intractable form, numerical results are provided. In a similar way, substituting (17) into (19), the following integral expression, which is (46), can be obtained. The first integral expression can be solved with the help of [43, Eq. (3.326.2[10])] and the second integral expression is numerically evaluated due to the intractable form.

$$\bar{P}_{e\,\gamma_{x_1}}^{\mathrm{S_2up}} = \frac{1}{2\sqrt{\pi}}\Bigg[\int_0^{\infty} \gamma_{th}^{-\frac{1}{2}} \exp\left(-\gamma_{\mathrm{th}}\right) \mathrm{d}\gamma_{\mathrm{th}} - \int_0^{\infty} \gamma_{\mathrm{th}}^{-\frac{1}{2}} \mathrm{e}^{-\gamma_{\mathrm{th}}\left(\frac{2\varphi+2(\beta_1+\beta_2)}{\varphi(\alpha_1-\gamma_{\mathrm{th}}\alpha_2)\mathrm{P_{s1}\Omega_h}}+\frac{2(\alpha_1+\alpha_2)}{\varphi\alpha_1\mathrm{P_{s2}\Omega_g}}+1\right)}$$
$$\times \frac{1}{P_{s2}\Omega_c}\left(\frac{\gamma_{\mathrm{th}}\left(\beta_1+\beta_2\right)}{\varphi\left(\alpha_1-\gamma_{th}\alpha_2\right)P_{s1}\Omega_h}+\frac{\left(\alpha_1+\alpha_2\right)\gamma_{\mathrm{th}}}{\varphi\alpha_1 P_{s2}\Omega_g}+\frac{1}{P_{s2}\Omega_c}\right)^{-1}\frac{1}{P_r\Omega_b}\left(\frac{\varphi\gamma_{\mathrm{th}}}{\varphi\left(\alpha_1-\gamma_{th}\alpha_2\right)P_{s1}\Omega_h}+\frac{1}{P_r\Omega_b}\right)^{-1} d\gamma_{th}\Bigg] \tag{46}$$

Likewise, substituting (16) into (22) the following expression can be obtained.

$$\bar{P}_{e\,\gamma_{y_2}}^{\mathrm{S_1up}} = \frac{1}{2\sqrt{\pi}}\Bigg[\int_0^{\infty} x^{-\frac{1}{2}} \exp\left(-\mathrm{x}\right) \mathrm{dx} - \int_0^{\infty} \mathrm{x}^{-\frac{1}{2}} \mathrm{e}^{-\mathrm{x}\left(1+\frac{2(\beta_1+\beta_2)}{\varphi\beta_2\mathrm{P_{s1}\Omega_h}}+\frac{2\varphi+2(\alpha_1+\alpha_2)}{\varphi\beta_2\mathrm{P_{s2}\Omega_g}}\right)}$$
$$\times\left(\frac{\left(\left(\beta_1+\beta_2\right)\varphi\beta_2 P_{s2}\Omega_g+\left(\alpha_1+\alpha_2\right)\varphi\beta_2 P_{s1}\Omega_h\right)P_{s1}\Omega_a}{\varphi^2\beta_2^2 P_{s2}\Omega_g P_{s1}\Omega_h}x+1\right)^{-1}\left(\frac{P_r\Omega_b}{\beta_2 P_{s2}\Omega_g}x+1\right)^{-1} dx\Bigg]. \tag{47}$$

With the help of [43, Eq. $(3.326.2^{10})$], the first integral can be solved as $\Gamma\left(\frac{1}{2}\right)$. By using the [41, Eq. (10, 11)], the second integral can be written as

$$\int_0^{\infty} x^{-\frac{1}{2}} G_{0,1}^{1,0}\left(x\left(1+\frac{2\left(\beta_1+\beta_2\right)}{\varphi\beta_2 P_{s1}\Omega_h}+\frac{2\varphi+2\left(\alpha_1+\alpha_2\right)}{\varphi\beta_2 P_{s2}\Omega_g}\right)\middle|\begin{matrix}-\\0\end{matrix}\right)$$
$$\times G_{1,1}^{1,1}\left(x\left(\frac{\left(\left(\beta_1+\beta_2\right)\varphi\beta_2 P_{s2}\Omega_g+\left(\alpha_1+\alpha_2\right)\varphi\beta_2 P_{s1}\Omega_h\right)P_{s1}\Omega_a}{\varphi^2\beta_2^2 P_{s2}\Omega_g P_{s1}\Omega_h}\right)\middle|\begin{matrix}0\\0\end{matrix}\right) G_{1,1}^{1,1}\left(x\left(\frac{P_r\Omega_b}{\beta_2 P_{s2}\Omega_g}\right)\middle|\begin{matrix}0\\0\end{matrix}\right) dx. \tag{48}$$

With the help of [42, Eq. (13)], the integral expression in (48) can be solved as

$$\left(1+\frac{2\left(\beta_1+\beta_2\right)}{\varphi\beta_2 P_{s1}\Omega_h}+\frac{2\varphi+2\left(\alpha_1+\alpha_2\right)}{\varphi\beta_2 P_{s2}\Omega_g}\right)^{-\frac{1}{2}}$$
$$\times G_{1,0:1,1:1,1}^{1,0:1,1:1,1}\left(\begin{matrix}\frac{1}{2}\\-\end{matrix}\middle|\begin{matrix}0\\0\end{matrix}\middle|\begin{matrix}0\\0\end{matrix}\middle|\frac{\left(\frac{\left(\left(\beta_1+\beta_2\right)\varphi\beta_2 P_{s2}\Omega_g+\left(\alpha_1+\alpha_2\right)\varphi\beta_2 P_{s1}\Omega_h\right)P_{s1}\Omega_a}{\varphi^2\beta_2^2 P_{s2}\Omega_g P_{s1}\Omega_h}\right)}{\left(1+\frac{2(\beta_1+\beta_2)}{\varphi\beta_2 P_{s1}\Omega_h}+\frac{2\varphi+2(\alpha_1+\alpha_2)}{\varphi\beta_2 P_{s2}\Omega_g}\right)},\frac{\left(\frac{P_r\Omega_b}{\beta_2 P_{s2}\Omega_g}\right)}{\left(1+\frac{2(\beta_1+\beta_2)}{\varphi\beta_2 P_{s1}\Omega_h}+\frac{2\varphi+2(\alpha_1+\alpha_2)}{\varphi\beta_2 P_{s2}\Omega_g}\right)}\right). \tag{49}$$

The α term is set to $\frac{1}{2}$ in [42, Eq. (13)]. Likewise, $\bar{P}_{e\,\gamma_{x_1}}^{\mathrm{S_2up}}$ can be calculated as

$$\bar{P}_{e\,\gamma_{x_2}}^{\mathrm{S_2up}} = \frac{1}{2\sqrt{\pi}}\Bigg[\Gamma\left(\frac{1}{2}\right)-\left(1+\frac{2\varphi+2\left(\beta_1+\beta_2\right)}{\varphi\alpha_2 P_{s1}\Omega_h}+\frac{2\left(\alpha_1+\alpha_2\right)}{\varphi\alpha_2 P_{s2}\Omega_g}\right)^{-\frac{1}{2}}$$
$$\times G_{1,0:1,1:1,1}^{1,0:1,1:1,1}\left(\begin{matrix}\frac{1}{2}\\-\end{matrix}\middle|\begin{matrix}0\\0\end{matrix}\middle|\begin{matrix}0\\0\end{matrix}\middle|\frac{\left(\frac{\left(\left(\beta_1+\beta_2\right)\varphi\alpha_2 P_{s2}\Omega_g+\left(\alpha_1+\alpha_2\right)\varphi\alpha_2 P_{s1}\Omega_h\right)P_{s2}\Omega_c}{\varphi^2\alpha_2^2 P_{s2}\Omega_g P_{s1}\Omega_h}\right)}{\left(1+\frac{2\varphi+2(\beta_1+\beta_2)}{\varphi\alpha_2 P_{s1}\Omega_h}+\frac{2(\alpha_1+\alpha_2)}{\varphi\alpha_2 P_{s2}\Omega_g}\right)},\frac{\left(\frac{P_r\Omega_b}{\alpha_2 P_{s1}\Omega_h}\right)}{\left(1+\frac{2\varphi+2(\beta_1+\beta_2)}{\varphi\alpha_2 P_{s1}\Omega_h}+\frac{2(\alpha_1+\alpha_2)}{\varphi\alpha_2 P_{s2}\Omega_g}\right)}\right)\Bigg]. \tag{50}$$

Substituting (15) into (24), the following expression can be obtained.

$$ER_{\gamma_{y_1}}^{\mathrm{S_1up}} = \frac{1}{ln2}\int_0^{\infty} e^{-\gamma_{th}\left(\frac{2(\beta_1+\beta_2)}{\varphi\beta_2 P_s\Omega_h}+\frac{2\varphi+2(\alpha_1+\alpha_2)}{\varphi(\beta_2-\gamma_{th}\beta_1)P_s\Omega_g}\right)}\frac{1}{P_s\Omega_a}\left(\frac{\left(\beta_1+\beta_2\right)\gamma_{\mathrm{th}}}{\varphi\beta_2 P_s\Omega_h}+\frac{\left(\alpha_1+\alpha_2\right)\gamma_{\mathrm{th}}}{\varphi\left(\beta_2-\gamma_{th}\beta_1\right)P_s\Omega_g}+\frac{1}{P_s\Omega_a}\right)^{-1}$$
$$\times\frac{1}{P_r\Omega_b}\left(\frac{\varphi\gamma_{\mathrm{th}}}{\varphi\left(\beta_2-\gamma_{th}\beta_1\right)P_s\Omega_g}+\frac{1}{P_r\Omega_b}\right)^{-1}\left(1+\gamma_{th}\right)^{-1} d\gamma_{\mathrm{th}}. \tag{51}$$

Since the integral expression in (51) has an intractable form, $ER_{\gamma_{y_1}}^{S_1up}$ is numerically evaluated. Likewise, $ER_{\gamma_{x_1}}^{S_2up}$, which is presented below, is also numerically evaluated

$$ER_{\gamma_{x_1}}^{S_2up} = \frac{1}{ln2}\int_0^{\infty} e^{-\gamma_{th}\left(\frac{2\varphi+2(\beta_1+\beta_2)}{\varphi(\alpha_1-\gamma_{th}\alpha_2)P_{s1}\Omega_h}+\frac{2(\alpha_1+\alpha_2)}{\varphi\alpha_1 P_{s2}\Omega_g}\right)}\frac{1}{P_{s2}\Omega_c}\left(\frac{\gamma_{\text{th}}(\beta_1+\beta_2)}{\varphi(\alpha_1-\gamma_{th}\alpha_2)P_{s1}\Omega_h}+\frac{(\alpha_1+\alpha_2)\gamma_{\text{th}}}{\varphi\alpha_1 P_{s2}\Omega_g}+\frac{1}{P_{s2}\Omega_c}\right)^{-1}$$
$$\times\frac{1}{P_r\Omega_b}\left(\frac{\varphi\gamma_{\text{th}}}{\varphi(\alpha_1-\gamma_{th}\alpha_2)P_{s1}\Omega_h}+\frac{1}{P_r\Omega_b}\right)^{-1}(1+\gamma_{th})^{-1}d\gamma_{\text{th}}. \tag{52}$$

Regarding $ER_{\gamma_{y_2}}^{S_1up}$, substituting the related CDF expressions into the ER formula, which is presented in (16), the following integral expression can be obtained.

$$\text{ER}_{\gamma_{y_2}}^{S_1up} = \frac{1}{\ln 2}\int_0^{\infty} \text{e}^{-\text{x}\left(\frac{2(\beta_1+\beta_2)}{\varphi\beta_2 P_{s1}\Omega_h}+\frac{2\varphi+2(\alpha_1+\alpha_2)}{\varphi\beta_2 P_{s2}\Omega_g}\right)}\left(\frac{\left((\beta_1+\beta_2)\varphi\beta_2 P_{s2}\Omega_g+(\alpha_1+\alpha_2)\varphi\beta_2 P_{s1}\Omega_h\right)P_{s1}\Omega_a}{\varphi^2\beta_2^2 P_{s1}\Omega_h P_{s2}\Omega_g}\text{x}+1\right)^{-1}$$
$$\times\left(\frac{P_r\Omega_b}{\beta_2 P_{s2}\Omega_g}x+1\right)^{-1}(1+x)^{-1}dx\Bigg]. \tag{53}$$

By using partial fraction decomposition technique the integral expression in (53) can be written as:

$$ER_{\gamma_{y_2}}^{S_1up} = \frac{1}{ln2}\int_0^{\infty} e^{-x\left(\frac{2(\beta_1+\beta_2)}{\varphi\beta_2 P_{s1}\Omega_h}+\frac{2\varphi+2(\alpha_1+\alpha_2)}{\varphi\beta_2 P_{s2}\Omega_g}\right)}\Bigg[\Psi\Bigg]dx$$
$$= \frac{1}{\ln 2}\int_0^{\infty} \text{e}^{-\text{x}\left(\frac{2(\beta_1+\beta_2)}{\varphi\beta_2 P_{s1}\Omega_h}+\frac{2\varphi+2(\alpha_1+\alpha_2)}{\varphi\beta_2 P_{s2}\Omega_g}\right)}\Bigg[\Theta\Bigg]\text{dx}, \tag{54}$$

where $\Psi = \left[\frac{1}{\left(\frac{((\beta_1+\beta_2)\varphi\beta_2 P_{s2}\Omega_g+(\alpha_1+\alpha_2)\varphi\beta_2 P_{s1}\Omega_h)P_{s1}\Omega_a}{\varphi^2\beta_2^2 P_{s1}\Omega_h P_{s2}\Omega_g}x+1\right)\left(\frac{P_r\Omega_b}{\beta_2 P_{s2}\Omega_g}x+1\right)(1+x)}\right]$ and $\Theta = \Bigg[\frac{B_1}{\left(\frac{((\beta_1+\beta_2)\varphi\beta_2 P_{s2}\Omega_g+(\alpha_1+\alpha_2)\varphi\beta_2 P_{s1}\Omega_h)P_{s1}\Omega_a}{\varphi^2\beta_2^2 P_{s1}\Omega_h P_{s2}\Omega_g}x+1\right)}+$
$\frac{B_2}{\left(\frac{P_r\Omega_b}{\beta_2 P_{s2}\Omega_g}x+1\right)}+\frac{B_3}{(1+x)}\Bigg]$, $B_1 = \lim\limits_{x\to-\frac{\varphi^2\beta_2^2 P_{s1}\Omega_h P_{s2}\Omega_g}{((\beta_1+\beta_2)\varphi\beta_2 P_{s2}\Omega_g+(\alpha_1+\alpha_2)\varphi\beta_2 P_{s1}\Omega_h)P_{s1}\Omega_a}}\times$
$\frac{\partial}{\partial x}\left(\frac{\left((\beta_1+\beta_2)\varphi\beta_2 P_{s2}\Omega_g+(\alpha_1+\alpha_2)\varphi\beta_2 P_{s1}\Omega_h\right)P_{s1}\Omega_a}{\varphi^2\beta_2^2 P_{s1}\Omega_h P_{s2}\Omega_g}x+1\right)[\Psi]$, $B_2 = \lim\limits_{x\to-\frac{\beta_2 P_{s2}\Omega_g}{P_r\Omega_b}}\frac{\partial}{\partial x}\left(\frac{P_r\Omega_b}{\beta_2 P_{s2}\Omega_g}x+1\right)[\Psi]$, and
$B_3 = \lim\limits_{x\to-1}\frac{\partial}{\partial x}(x+1)[\Psi]$. Utilizing distributive properties and [41, Eq. (10, 11)] and also solving the integral expressions with the help of [41, Eq. (21)], the final expression can be obtained. Likewise, substituting (18) into the ER formula and following the same procedures as in $\text{ER}_{\gamma_{y_2}}^{S_1up}$, the final expression can be obtained as in (23). The α is set to 1 in [41, Eq. (21)]. Also note that $B_4 = \lim\limits_{x\to-\frac{\varphi^2\alpha_2^2 P_{s1}\Omega_h P_{s2}\Omega_g}{((\beta_1+\beta_2)\varphi\alpha_2 P_{s2}\Omega_g+(\alpha_1+\alpha_2)\varphi\alpha_2 P_{s1}\Omega_h)P_{s2}\Omega_c}}\times$
$\frac{\partial}{\partial x}\left(\frac{\left((\beta_1+\beta_2)\varphi\alpha_2 P_{s2}\Omega_g+(\alpha_1+\alpha_2)\varphi\alpha_2 P_{s1}\Omega_h\right)P_{s2}\Omega_c}{\varphi^2\alpha_2^2 P_{s1}\Omega_h P_{s2}\Omega_g}x+1\right)[T]$, $B_5 = \lim\limits_{x\to-\frac{\alpha_2 P_{s1}\Omega_h}{P_r\Omega_b}}\frac{\partial}{\partial x}\left(\frac{P_r\Omega_b}{\alpha_2 P_{s1}\Omega_h}x+1\right)[T]$, $B_6 =$
$\lim\limits_{x\to-1}\frac{\partial}{\partial x}(x+1)[T]$, and $T = \left[\frac{1}{\left(\frac{((\beta_1+\beta_2)\varphi\alpha_2 P_{s2}\Omega_g+(\alpha_1+\alpha_2)\varphi\alpha_2 P_{s1}\Omega_h)P_{s2}\Omega_c}{\varphi^2\alpha_2^2 P_{s1}\Omega_h P_{s2}\Omega_g}x+1\right)}\frac{1}{\left(\frac{P_r\Omega_b}{\alpha_2 P_{s1}\Omega_h}x+1\right)(1+x)}\right]$. In a similar way, $\text{ER}_{\gamma_{x_2}}^{S_2up}$ can be obtained as in (24).

REFERENCES

[1] Y. Saito *et al.*, "Non-orthogonal multiple access (noma) for cellular future radio access," *2013 IEEE 77th Vehic. Techn. Conf. (VTC Spring)*, pp. 1–5, 2013.

[2] O. Abbasi and A. Ebrahimi, "Cooperative noma with full-duplex amplify-and-forward relaying," *Trans. on Emerging Telecomm. Techn.*, vol. 29, no. 7, p. e3421, 2018, e3421 ett.3421. [Online]. Available: https://onlinelibrary.wiley.com/doi/abs/10.1002/ett.3421

[3] S. Singh and M. Bansal, "Performance analysis of non-orthogonal multiple access assisted cooperative relay system with channel estimation errors and imperfect successive interference cancellation," *Trans. on Emerging Telecomm. Techn.*, vol. n/a, no. n/a, p. e4374. [Online]. Available: https://onlinelibrary.wiley.com/doi/abs/10.1002/ett.4374

[4] M. Toka *et al.*, "Performance analyses of tas/alamouti-mrc noma in dual-hop full-duplex af relaying networks," 2021.

[5] V. Ozduran, N. Huda Mahmood, and H. Chergui, "Power-domain non-orthogonal multiple access based full-duplex one-way wireless relaying network," *Trans. on Emerging Telecomm. Techn.*, vol. n/a, no. n/a, p. e4276. [Online]. Available: https://onlinelibrary.wiley.com/doi/abs/10.1002/ett.4276

[6] S. Katti *et al.*, "XORs in the air: Practical wireless network coding," *IEEE/ACM Trans. on Networking*, vol. 16, no. 3, pp. 497–510, 2008.

[7] C. Y. Ho and C. Y. Leow, "Cooperative non-orthogonal multiple access using two-way relay," *2017 IEEE Intern. Conf. on Signal and Image Process. App. (ICSIPA)*, pp. 459–463, Sept 2017.

[8] A. Agarwal and A. K. Jagannatham, "Performance analysis for non-orthogonal multiple access (noma)-based two-way relay communication," *IET Communications*, vol. 13, pp. 363–370(7), March 2019.

[9] C. Y. Ho, C. Y. Leow, and Z. Ding, "Two-way relay assisted non-orthogonal multiple access," *Computer Commun.*, vol. 145, pp. 335–344, 2019.

[10] X. Wang *et al.*, "Exploiting full-duplex two-way relay cooperative non-orthogonal multiple access," *IEEE Trans. on Commun.*, vol. 67, no. 4, pp. 2716–2729, 2019.

[11] C. Zhong and Z. Zhang, "Non-orthogonal multiple access with cooperative full-duplex relaying," *IEEE Commun. Letters*, vol. 20, no. 12, pp. 2478–2481, 2016.

[12] M. Shokair, W. Saad, and S. M. Ibraheem, "On the achievable capacity of one-way noma based bi-directional full-duplex relay assisted cooperative networks," *2018 35th National Radio Science Conference (NRSC)*, pp. 130–139, 2018.

[13] X. Yue *et al.*, "Outage performance of two-way relay non-orthogonal multiple access systems," *2018 IEEE Intern. Conf. on Commun. (ICC)*, pp. 1–6, 2018.

[14] ——, "Modeling and analysis of two-way relay non-orthogonal multiple access systems," *IEEE Trans. on Commun.*, vol. 66, no. 9, pp. 3784–3796, 2018.

[15] T. T. T. Dao and P. N. Son, "Uplink non-orthogonal multiple access protocol in two-way relaying networks: realistic operation and performance analysis," *2020 7th NAFOSTED Conference on Information and Computer Science (NICS)*, pp. 399–404, 2020.

[16] X. Tian *et al.*, "I/q imbalance and imperfect sic on two-way relay noma systems," *Electronics*, vol. 9, no. 2, 2020.

[17] R. K. Ahiadormey, P. Anokye, S.-H. Park, and K.-J. Lee, "Two-way relaying non-orthogonal multiple access with imperfect successive interference cancellation in power line communications," *IEEE Open Journal of the Commun. Society*, vol. 1, pp. 1872–1885, 2020.

[18] D. Do *et al.*, "Throughput analysis of multipair two-way replaying networks with noma and imperfect csi," *IEEE Access*, vol. 8, pp. 128 942–128 953, 2020.

[19] Y. Xu, J. Cheng, G. Wang, and V. C. Leung, "Adaptive coordinated direct and relay transmission for noma networks: A joint downlink-uplink scheme," *IEEE Trans. on Wireless Commun.*, pp. 1–1, 2021.

[20] M. F. Kader, M. B. Uddin, M. A. L. Sarker, and S. Y. Shin, "Bidirectional relaying using non-orthogonal multiple access," *Physical Commun.*, vol. 33, pp. 266–274, 2019.

[21] J. Bae and Y. Han, "Joint power and time allocation for two-way cooperative noma," *IEEE Trans. on Vehic. Techn.*, vol. 68, no. 12, pp. 12 443–12 447, 2019.

[22] O. Ozdemir, "Achievable rate analysis for two-way relay non-orthogonal multiple access systems," *2021 IEEE Asia Pacific Conf. on Wireless and Mobile (APWiMob)*, pp. 80–85, 2021.

[23] S. Silva, G. A. A. Baduge, M. Ardakani, and C. Tellambura, "Noma-aided multi-way massive mimo relaying," *IEEE Trans. on Commun.*, vol. 68, no. 7, pp. 4050–4062, 2020.

[24] S. Potula, A. Sharma, K. R. Santhamgari, and S. R. Ijjada, "Outage analysis of half-duplex decode-and-forward relaying with cooperative noma in vehicular networks," *Materials Today: Proceedings*, 2021.

[25] M. K. Shukla, H. H. Nguyen, and O. J. Pandey, "Secrecy performance analysis of two-way relay non-orthogonal multiple access systems," *IEEE Access*, vol. 8, pp. 39 502–39 512, 2020.

[26] T.-L. Nguyen and D.-T. Do, "Outage performance analysis of full-duplex assisted non-orthogonal multiple access with bidirectional relaying mode," *Intern. Journal of Commun. Networks and Distributed Systems*, vol. 26, no. 4, pp. 398–408, 2021.

[27] T.-T. T. Nguyen and D.-T. Do, "Exploiting performance of two-way non-orthogonal multiple access networks: Joint impact of co-channel interference, full-duplex/half-duplex mode and sic receiver," *Ad Hoc Networks*, vol. 97, p. 102032, 2020. [Online]. Available: https://www.sciencedirect.com/science/article/pii/S1570870519300538

[28] V. Goutham and V. Harigovindan, "Full-duplex cooperative relaying with noma for the performance enhancement of underwater acoustic sensor networks," *Engineering Science and Technology, an Intern. Journal*, 2021.

[29] T. N. Do, D. B. da Costa, T. Q. Duong, and B. An, "Improving the performance of cell-edge users in noma systems using cooperative relaying," *IEEE Trans. on Commun.*, vol. 66, no. 5, pp. 1883–1901, 2018.

[30] S. Sadeghi, M. Mohammadi, and Z. Mobini, "Outage probability analysis of wireless-powered full-duplex cognitive non-orthogonal multiple access relaying systems," *2020 28th Iranian Conf. on Electrical Engineering (ICEE)*, pp. 1–6, 2020.

[31] Z. Xu, S. Wang, D. Liu, and Z. Wen, "Joint beamforming and power-splitting optimization for swipt-enabled miso full-duplex two-way cooperative noma systems," *Physical Commun.*, vol. 45, p. 101257, 2021. [Online]. Available: https://www.sciencedirect.com/science/article/pii/S1874490720303347

[32] G. Li, "A spectral efficient noma-based two-way relaying scheme for wireless networks with two relays," *KSII Trans. on Internet and Inform. Systems*, vol. 15, no. 1, pp. 365–382, Jan. 2021.

[33] Z. Fang *et al.*, "New noma-based two-way relay networks," *IEEE Trans. on Vehic. Techn.*, vol. 69, no. 12, pp. 15 314–15 324, 2020.

[34] L. Lv *et al.*, "Multi-antenna two-way relay based cooperative noma," *IEEE Trans. on Wireless Commun.*, vol. 19, no. 10, pp. 6486–6503, 2020.

[35] L. Lv *et al.*, "On the design of noma assisted multi-antenna two-way relay systems," *ICC 2020 - 2020 IEEE Intern. Conf. on Commun. (ICC)*, pp. 1–6, 2020.

[36] P. N. Son and T-T.T.Duy, "A new approach for two-way relaying networks: improving performance by successive interference cancellation, digital network coding and opportunistic relay selection," *Wireless Netw.*, vol. 26, pp. 1315–1329, 2020.

[37] M. V. T. Huynh, P. N. Son, "Exact outage probability of two-way decode-and-forward noma scheme with opportunistic relay selection," *KSII Trans. on Internet and Inform. Systems*, vol. 13, pp. 5862–5887, 2019.

[38] X. Tang *et al.*, "On the performance of two-way multiple relay non-orthogonal multiple access-based networks with hardware impairments," *IEEE Access*, vol. 7, pp. 128 896–128 909, 2019.

[39] T.-T. Dao and P. Son, "Cancel-decode-encode processing on two-way cooperative noma schemes in realistic conditions," *Wireless Commun. and Mobile Computing*, vol. 2021, pp. 1–15, 2021.

[40] B. Zheng, X. Wang, M. Wen, and F. Chen, "Noma-based multi-pair two-way relay networks with rate splitting and group decoding," *IEEE Journal on Selected Areas in Commun.*, vol. 35, no. 10, pp. 2328–2341, Oct 2017.

[41] V. S. Adamchik and O. I. Marichev, *The algorithm for calculating integrals of hypergeometric type functions and its realization in REDUCE systems*. Proc. Conf. ISSAC'90, Tokyo, pp. 212–224, 1990.

[42] N. H. Mahmood *et al.*, "Physical-layer security with full-duplex transceivers and multiuser receiver at eve," *IEEE Trans. on Commun.*, vol. 65, no. 10, pp. 4392–4405, Oct 2017.

[43] I. S. Gradshteyn and I. M. Ryzhik, *Tables of Integrals, Series and Products*. Elsevier Inc., 7th edition, 2007.

[44] E. Soleimani-Nasab, M. Matthaiou, M. Ardebilipour, and G. K. Karagiannidis, "Two-way AF relaying in the presence of co-channel interference," *IEEE Trans. on Commun.*, vol. 61, no. 8, pp. 3156–3169, August 2013.

[45] S. S. Ikki and S. Aissa, "Performance analysis of two-way amplify-and-forward relaying in the presence of co-channel interferences," *IEEE Trans. on Commun.*, vol. 60, no. 4, pp. 933–939, April 2012.

[46] L. Yang, K. Qaraqe, E. Serpedin, and M. S. Alouini, "Performance analysis of amplify-and-forward two-way relaying with co-channel interference and channel estimation error," *2013 IEEE Wireless Commun. and Netw. Conf. (WCNC)*, pp. 3710–3714, April 2013.

[47] T. Nguyen, H. H. K. Duy, H. Nguyen, and M. Voznak, "Throughput analysis in relaying cooperative systems considering time-switching with noma," *2018 41st Intern. Conf. on Telecommun. and Signal Processing (TSP)*, pp. 1–4, July 2018.

[48] Wolfram, *The Wolfram Functions Site [Online] Available: http://functions.wolfram.com/07.34.03.0392.01*, 2019.

[49] ——, *The Wolfram Functions Site [Online] Available: http://functions.wolfram.com/07.33.06.0012.01*, 2019.

[50] L. Jimenez Rodriguez, N. H. Tran, and T. Le-Ngoc, "Performance of full-duplex af relaying in the presence of residual self-interference," *IEEE J. on Selec. Areas in Commun.*, vol. 32, no. 9, pp. 1752–1764, 2014.

[51] A. Papoulis and U. Pillai, *Probability, random variables and stochastic processes*, 4th ed. McGraw-Hill, 11 2001.